



Article

On the Analysis of a Fractional Tuberculosis Model with the Effect of an Imperfect Vaccine and Exogenous Factors under the Mittag–Leffler Kernel

Saeed Ahmad ¹ , Sedat Pak ^{2,*} , Mati ur Rahman ^{3,4,*} and Afrah Al-Bossly ⁵

- ¹ Department of Mathematics, University of Malakand, Dir(L), Khyber Pakhtunkhwa 18800, Pakistan
- ² Department of Mathematics and Computer Sciences, Faculty of Science, Necmettin Erbakan University, Konya 42090, Türkiye
- ³ School of Mathematical Science, Shanghai Jiao Tong University, Shanghai 200240, China
- ⁴ Department of Computer Science and Mathematics, Lebanese American University, Beirut 1102-2801, Lebanon
- ⁵ Department of Mathematics, College of Science and Humanities in Al-Kharj, Prince Sattam Bin Abdulaziz University, Al-Kharj 11942, Saudi Arabia
- * Correspondence: spak@erbakan.edu.tr (S.P.); matimaths374@gmail.com (M.u.R.)

Abstract: This research study aims to investigate the effects of vaccination on reducing disease burden by analyzing a complex nonlinear ordinary differential equation system. The study focuses on five distinct sub-classes within the system to comprehensively explore the impact of vaccination. Specifically, the mathematical model employed in this investigation is a fractional representation of tuberculosis, utilizing the Atangana–Baleanu fractional derivative in the Caputo sense. The validity of the proposed model is established through a rigorous qualitative analysis. The existence and uniqueness of the solution are rigorously determined by applying the fundamental theorems of the fixed point approach. The stability analysis of the model is conducted using the Ulam–Hyers approach. Additionally, the study employs the widely recognized iterative Adams–Bashforth technique to obtain an approximate solution for the suggested model. The numerical simulation of the tuberculosis model is comprehensively discussed, with a particular focus on the assumptions made regarding vaccination. The model assumes that only a limited portion of the population is vaccinated at a steady rate, and the efficacy of the vaccine is a critical factor in reducing disease burden. The findings of the study indicate that the proposed model can effectively assess the impact of vaccination on mitigating the spread of tuberculosis. Furthermore, the numerical simulation underscores the significance of vaccination as an effective control measure against tuberculosis.

Keywords: SVEIR TB model; qualitative analysis; stability analysis; ABC fractional derivative; Adam–Bashforth method; numerical simulation



Citation: Ahmad, S.; Pak, S.; Rahman, M.u.; Al-Bossly, A. On the Analysis of a Fractional Tuberculosis Model with the Effect of an Imperfect Vaccine and Exogenous Factors under the Mittag–Leffler Kernel. *Fractal Fract.* **2023**, *7*, 526. <https://doi.org/10.3390/fractalfract7070526>

Academic Editor: Ivanka Stamova

Received: 29 May 2023

Revised: 21 June 2023

Accepted: 29 June 2023

Published: 3 July 2023



Copyright: © 2023 by the authors. Licensee MDPI, Basel, Switzerland. This article is an open access article distributed under the terms and conditions of the Creative Commons Attribution (CC BY) license (<https://creativecommons.org/licenses/by/4.0/>).

1. Introduction

Tuberculosis (TB) is a prevalent and highly transmissible respiratory illness that remains a significant global health concern, being responsible for a substantial number of fatalities. This contagious disease predominantly targets the pulmonary system in humans, but can also affect various other vital organs including the kidneys, brain, spine, and central nervous system [1–3]. TB is primarily caused by an acid-resistant bacillus bacterium known as *Mycobacterium tuberculosis*. This pathogenic microorganism was first identified and characterized by Dr. Robert Koch in 1882 [4]. In the year 2019, tuberculosis (TB) tragically resulted in the loss of approximately 1.5 million lives on a global scale. The burden of TB remains significant, despite the availability of efficient treatments and preventive measures, with an estimated ten million people infected globally. This includes 5.60 million men, 3.20 million women, and 1.2 million children. Tuberculosis bacteria are pervasive and have the potential to infect individuals across all age groups. Recognizing the urgent

need to address this highly transmissible disease, the World Health Organization has set a target to eliminate TB worldwide by the year 2030. This ambitious goal reflects the global commitment to combating TB and underscores the importance of concerted efforts on the prevention, diagnosis, and treatment for achieving this objective (WHO, 14 October 2020). TB often remains in an asymptomatic state for prolonged periods, with the bacteria residing in a dormant state within the body. This extended period of dormancy poses challenges in understanding the transition from latent to active TB disease. Individuals with weakened immune systems are more vulnerable to contracting TB through contact with infectious individuals. Low-income countries such as Pakistan, South Africa, and Nigeria have a high death rate due to the expensive and lengthy medications required to treat TB. Pakistan ranks fifth among the twenty two high-burden countries, with approximately 65 percent of reported cases [5–7]. Treatment for TB involves a six-month course of four antimicrobial drugs, which can completely cure the disease. Bacillus Calmette–Guerin (BCG) is a highly effective vaccine in children, providing over 50% protection against lung infection and more than 80% protection against all types of TB. However, its efficacy in adults is limited [8–10].

Previous studies [11–13] have investigated the impact of exogenous factors and the effectiveness of imperfect vaccines in tuberculosis (TB) epidemics through the application of mathematical models. Bhunu et al. [14] have expanded the TB model to include the aspect of exogenous reinfection and relapse of the disease, as well as chemoprophylaxis and treatment of infection in various stages. In [15], the authors presented a TB transmission model with exogenous reinfection and investigated if the proposed system is subject to Hopf bifurcation. They also found the direction of the Hopf bifurcation and the stability of the periodic bifurcation solution. Additionally, Ullah et al. [16] have studied the dynamics of tuberculosis transmission in the KP province of Pakistan. The problem addressed in this research study was parameterized by utilizing authentic data obtained from the national TB control program covering the time period from 2002 to 2017. The stability analysis of the model was performed using basic reproductive numbers, and the results showed that the model is globally and locally stable. In another study by [17], a TB model was developed and analyzed with a nonlinear incidence rate and exogenous reinfection. The threshold parameter was found to be crucial in epidemiology for determining the persistence or extinction of infectious diseases. Two types of bifurcation and stability criteria were discussed in this study. The use of fractional calculus was also highlighted for modeling real-world phenomena related to biological, physical, and engineering problems [18–22].

The utilization of fractional calculus has gained significant traction among researchers and mathematicians, owing to its capacity to offer a more precise depiction of natural phenomena compared to conventional integral order differential equations. Fractional integrals and derivatives have wide-ranging applications in various fields of science and engineering [23]. For example, fractional calculus can be used to model controllability [24], chaotic systems [25], financial modeling [26], diffusion processes, vibrations [27,28], and many other complex phenomena. Atangana and Baleanu [29] presented a new definition for fractional differential and addressed the calculus challenge of whether it is possible to construct another fractional derivative that has a non-singular kernel. They mentioned that fractional calculus can better describe the dynamics of nonlocal phenomena in some cases. This new definition uses the kernel to represent a non-local and non-singular kernel called the Mittag–Leffler function. Using this function in modern fractional calculus explains the hidden aspect of a nonlocal dynamical system. From a numerical point of view, fractional calculus is more easily used based on the nonsingular ML kernel [30]. The ML function is highly used and useful in fractional calculus. Pskhu [31] proposed an important part of the definition for different fractional differentials. Several researchers have been working on fractional differential equations and applying them to real-world problems such as biological, mechanical, control, and financial systems problems [32–35].

Several applications of this new AB derivative have been explored in diverse fields such as the theory of chaos [36], variational problems [37], heat transfer [38] and many more [39,40]. Furthermore, it is imperative to engage in a comprehensive discussion re-

garding the aforementioned equation in conjunction with the fractional integrator. This novel operator holds significant relevance in the realm of control theory, as well as in the context of fractional variational Euler, Lagrange, and Hamilton equations [41,42]. In recent studies, some basic properties of the newly presented AB differentiable have been shown, for instance, in [43] established the Laplace transform formulae for AB differentiable, in [44] presented integration by parts and Euler Lagrange equations. Furthermore, some other more useful and effective studies of the fractional derivatives are applied in mathematical formulation to many real-world problems [45–49]. Researchers have used a variety of operators to explore and analyze fractional differential equations, and some groundbreaking work has been published in the literature on these equations. Each operator has distinctive qualities and advantages that make them suited for various applications and fractional derivative-related problem formulations. Several publications have advanced our knowledge of fractional calculus and its uses in a variety of disciplines, including [50–54].

Our study has focused on the analysis of a nonlinear system of ordinary differential equations (ODEs) comprising five compartments: susceptible population \mathbb{S} , vaccinated class \mathbb{V} , exposed class \mathbb{E} , infected class \mathbb{I} , and recovered class \mathbb{R} taken from [55]. In this study, we have introduced a new fractional version of this system using the fractional derivative operator ABC with a fractional order $0 < h \leq 1$.

$$\begin{aligned}
 ABC \mathbf{D}_t^h(\mathbb{S}(t)) &= \Theta + \vartheta \mathbb{V} - \zeta \mathbb{S} - \alpha_1 \mathbb{S} \mathbb{I} - d_1 \mathbb{S}, \\
 ABC \mathbf{D}_t^h(\mathbb{V}(t)) &= \zeta \mathbb{S} - \gamma_0 \alpha_1 \mathbb{V} \mathbb{I} - \vartheta \mathbb{V} - d_1 \mathbb{V}, \\
 ABC \mathbf{D}_t^h(\mathbb{E}(t)) &= \alpha_1 \mathbb{S} \mathbb{I} + \gamma_0 \alpha_1 \mathbb{V} \mathbb{I} - \pi \alpha_1 \mathbb{E} \mathbb{I} - (\varkappa + d_1) \mathbb{E} + \varsigma \alpha_1 \mathbb{I} \mathbb{R}, \\
 ABC \mathbf{D}_t^h(\mathbb{I}(t)) &= \pi \alpha_1 \mathbb{E} \mathbb{I} + \varkappa \mathbb{E} - (d_1 + \alpha_2 + d_2) \mathbb{I}, \\
 ABC \mathbf{D}_t^h(\mathbb{R}(t)) &= \alpha_2 \mathbb{I} - \varsigma \alpha_1 \mathbb{I} \mathbb{R} - d_1 \mathbb{R}, \\
 \mathbb{S}(0) = \mathbb{S}_0, \mathbb{V}(0) &= \mathbb{V}_0, \mathbb{E}(0) = \mathbb{E}_0, \mathbb{I}(0) = \mathbb{I}_0, \mathbb{R}(0) = \mathbb{R}_0.
 \end{aligned}
 \tag{1}$$

The positivity, feasibility, and stability of the examined system can be assessed by incorporating all compartments, as demonstrated in [55].

The parameters utilized in the proposed system are given Table 1.

Table 1. Description of the used parameters of model (1).

Value	Details
Θ	constant rate of birth
d_1	rate of diminished for each compartment
ϑ	the rate at which vaccine wanes over time
$\alpha_1 \mathbb{S} \mathbb{I}$	the rate at which class \mathbb{S} becomes infected
d_2	death rate of TB induced
ζ	the rate of vaccine at which \mathbb{S} moves to \mathbb{V}
α_1	the rate of transmission
α_2	the rate at which class \mathbb{I} become recovered
γ_0	the rate of viability of vaccine
π	rate of new infection
\varkappa	the rate at which class \mathbb{E} become infected
ς	the rate of low immunity

In this study, our investigation has focused on the application of a fractional approach to the tuberculosis (TB) model, encompassing five compartments and employing the Atangana–Baleanu–Caputo fractional operator. Our findings revealed the existence of a solution for the system, and for the IVP, we established the uniqueness of the solution within this fractional framework. In order to assess the stability of the solution, we employed the Ulam–Hyers concept, demonstrating its stability. To compute an approximate solution, we employed the Newton interpolation method, which incorporates a fractional parameter in the expression, thereby increasing the degree of freedom for numerical simulation of the five compartments. This continuous spectrum describes the total density that ranges between 0 and 1. The structure of this manuscript is as follows: in Section 2, we recall some

basic definitions and symbols from fractional calculus. In Section 3, we prove the theoretical results of the given model with the aid of fixed point theory. In the same section, we also discuss the UH stability by making a small change in the initial condition. In Section 4, we have used the famous Adams–Bashforth methods that exist in the literature to find the approximate solution for the considered model. The numerical simulation is also discussed to summarize our results in the same section by using MATLAB 16 to obtain the graphical results. Finally, in Section 5 we conclude our work.

2. Basic Results

Here, we show some basic notation and statement from fractional calculus [29].

Definition 1. Consider a function $\mathbf{U}(t) \in \mathfrak{h} \in [0, 1]$; then, the fractional operator in the sense of Caputo ABC is defined as

$${}^{ABC}\mathbf{D}_t^{\mathfrak{h}}(\mathbf{U}(t)) = \frac{\mathcal{M}(\mathfrak{h})}{1 - \mathfrak{h}} \int_0^t \mathbf{E}_{\mathfrak{h}} \left[\frac{-\mathfrak{h}}{1 - \mathfrak{h}} (t - u)^{\mathfrak{h}} \right] \frac{d}{du} \mathbf{U}(u) du, \quad (2)$$

where the normalization function $\mathcal{M}(0) = \mathcal{M}(1) = 1$ and $\mathbf{E}_{\mathfrak{h}}$ is the Mittag–Leffler function given by

$$\mathbf{E}_{\mathfrak{h}}(y) = \sum_{k=0}^{\infty} \frac{y^k}{\Gamma(\mathfrak{h}k + 1)}.$$

Definition 2. Consider a function $\mathbf{U}(t) \in L^1(0, T)$. The integral of ABC can be defined as

$${}^{ABC}\mathbf{I}_t^{\mathfrak{h}}\mathbf{U}(t) = \frac{1 - \mathfrak{h}}{\mathcal{M}(\mathfrak{h})} \mathbf{U}(t) + \frac{\mathfrak{h}}{\mathcal{M}(\mathfrak{h})} \frac{1}{\Gamma(\mathfrak{h})} \int_0^t (t - u)^{\mathfrak{h}-1} \mathbf{U}(u) du, \quad t > 0. \quad (3)$$

Lemma 1 ([29]). The solution of the given problem and for $\mathfrak{h} \in (0, 1]$, can be

$$\begin{aligned} {}^{ABC}\mathbf{D}_t^{\mathfrak{h}}\mathbf{U}(t) &= \mathbf{U}(t), \\ \mathbf{U}(t) &= \mathbf{U}_0, \end{aligned}$$

with the assumption

$$\mathbf{U}(t) = \mathbf{U}_0 + \frac{1 - \mathfrak{h}}{\mathcal{M}(\mathfrak{h})} \mathbf{U}(t) + \frac{\mathfrak{h}}{\mathcal{M}(\mathfrak{h})} \frac{1}{\Gamma(\mathfrak{h})} \int_0^t (t - u)^{\mathfrak{h}-1} \mathbf{U}(u) du. \quad (4)$$

3. Existence Theory

In this section, we examined the feasibility of the model in real-world scenarios. Additionally, we demonstrated the stability and existence results of the problem under consideration. Therefore, we rearrange the given problem as

$$\begin{cases} {}^{ABC}\mathbf{D}_t^{\mathfrak{h}}\mathbf{S}(t) &= \mathbf{G}_1(\mathbf{S}, \mathbf{V}, \mathbf{E}, \mathbf{I}, \mathbf{R}), \\ {}^{ABC}\mathbf{D}_t^{\mathfrak{h}}(\mathbf{V}(t)) &= \mathbf{G}_2(\mathbf{S}, \mathbf{V}, \mathbf{E}, \mathbf{I}, \mathbf{R}), \\ {}^{ABC}\mathbf{D}_t^{\mathfrak{h}}(\mathbf{E}(t)) &= \mathbf{G}_3(\mathbf{S}, \mathbf{V}, \mathbf{E}, \mathbf{I}, \mathbf{R}), \\ {}^{ABC}\mathbf{D}_t^{\mathfrak{h}}(\mathbf{I}(t)) &= \mathbf{G}_4(\mathbf{S}, \mathbf{V}, \mathbf{E}, \mathbf{I}, \mathbf{R}), \\ {}^{ABC}\mathbf{D}_t^{\mathfrak{h}}(\mathbf{R}(t)) &= \mathbf{G}_5(\mathbf{S}, \mathbf{V}, \mathbf{E}, \mathbf{I}, \mathbf{R}), \end{cases} \quad (5)$$

Writing Equation (1) in the form

$$\begin{aligned} {}^{ABC}\mathbf{D}_t^{\mathfrak{h}}\mathbf{U}(t) &= \eta(t, \mathbf{U}(t)), \\ \mathbf{U}(0) &= \mathbf{U}_0(t), \end{aligned} \quad (6)$$

where

$$\begin{cases} \mathbf{U}(t) := (\mathbb{S}, \mathbb{V}, \mathbb{E}, \mathbb{I}, \mathbb{R})^T, \\ \mathbf{U}_0 := (\mathbb{S}_0, \mathbb{V}_0, \mathbb{E}_0, \mathbb{I}_0, \mathbb{R}_0)^T, \\ \eta(t, \mathbf{U}(t)) := \mathbf{G}_i(t, \mathbb{S}, \mathbb{V}, \mathbb{E}, \mathbb{I}, \mathbb{R})^T, \quad i = 1, 2, \dots, 5, \end{cases} \tag{7}$$

where $(\cdot)^T$ defined the transpose of the vector. In view of Lemma 1, we obtain the following integral of equation from system (6) as

$$\mathbf{U}(t) = \mathbf{U}_0 + \frac{1 - \hbar}{\mathcal{M}(\hbar)} \mathbf{z}(t, \mathbf{U}(t)) + \frac{\hbar}{\mathcal{M}(\hbar)\Gamma(\hbar)} \int_0^t (t - \varphi)^{\hbar-1} \mathbf{z}(\varphi, \mathbf{U}(\varphi)) d\varphi. \tag{8}$$

Next, let a Banach space be $Y = C([0, T], \mathbf{R}^k)_{1 \leq k \leq n}$ under the norm $\|\mathbf{U}\| = \sup_{t \in [0, T]} |\mathbf{U}(t)|$. Further, $\Phi = (Y^5, \|\mathbf{U}\|)$ be a Banach space and

$$\|\mathbf{U}\| = \sup_{t \in [0, T]} (|\mathbb{S}| + |\mathbb{V}| + |\mathbb{E}| + |\mathbb{I}| + |\mathbb{R}|). \tag{9}$$

In the next theorem, we showed the existence results with the aid of Schauder’s fixed point theorem.

Theorem 1. Suppose $\mathbf{z} \in \Phi$ be a continuous and \exists a constant $\mathfrak{V} > 0 \ni |\mathbf{z}(t, \mathbf{U}(t))| \leq \mathfrak{V}(1 + \|\mathbf{U}\|)$, $\forall t \in [0, T]$ and $\mathbf{U} \in \Phi$; then,

$$\nabla_1 = \left(\frac{(1 - \hbar)\Gamma(\hbar)\mathfrak{V} + \mathfrak{V}T^\hbar}{\mathcal{M}(\hbar)\Gamma(\hbar)} \right) < 1. \tag{10}$$

The solution for the above Equation (8) is unique and continuous for all $t \in [0, T]$.

Proof. From Equation (10), the given problem solution is also a solution of the equivalent integral Equation (8). Suppose the operator $\mathcal{U} : \Phi \rightarrow \Phi$ is given by

$$(\mathcal{U}\mathbf{U})(t) = \mathbf{U}_0 + \frac{1 - \hbar}{\mathcal{M}(\hbar)} \mathbf{z}(t, \mathbf{U}(t)) + \frac{\hbar}{\mathcal{M}(\hbar)\Gamma(\hbar)} \int_0^t (t - \varphi)^{\hbar-1} \mathbf{z}(\varphi, \mathbf{U}(\varphi)) d\varphi. \tag{11}$$

A bounded closed and convex ball can be defined as $\mathbb{B}_\varrho = \{\mathbf{U} \in \Phi : \|\mathbf{U}\| \leq \varrho, \varrho > 0\}$ with $\varrho \geq \frac{\nabla_2}{1 - \nabla_1}$, where

$$\nabla_2 = |\mathbf{U}_0| + \frac{1 - \hbar}{\mathcal{M}(\hbar)} \mathfrak{V} + \frac{T^\hbar}{\mathcal{M}(\hbar)\Gamma(\hbar)} \mathfrak{V}. \tag{12}$$

It is sufficient to verify that $(\mathcal{U}\mathbb{B}_\varrho) \subset \mathbb{B}_\varrho, \forall t \in [0, T]$; then, we obtain

$$\begin{aligned} |(\mathcal{U}\mathbf{U})(t)| &\leq |\mathbf{U}_0| + \frac{1 - \hbar}{\mathcal{M}(\hbar)} |\mathbf{z}(t, \mathbf{U}(t))| + \frac{\hbar}{\mathcal{M}(\hbar)\Gamma(\hbar)} \int_0^t (t - \lambda)^{\hbar-1} |\mathbf{z}(\lambda, \mathbf{U}(\lambda))| d\lambda \\ &\leq |\mathbf{U}_0| + \frac{1 - \hbar}{\mathcal{M}(\hbar)} \mathfrak{V}(1 + \|\mathbf{U}(t)\|) + \frac{\hbar}{\mathcal{M}(\hbar)\Gamma(\hbar)} \int_0^t (t - \lambda)^{\hbar-1} \mathfrak{V}(1 + \|\mathbf{U}(\lambda)\|) d\lambda, \end{aligned} \tag{13}$$

and $\mathbf{U} \in \mathbb{B}_\varrho$. We also obtain

$$\begin{aligned} \|(\mathcal{U}\mathbf{U})\| &\leq |\mathbf{U}_0| + \frac{1 - \hbar}{\mathcal{M}(\hbar)} \mathfrak{V}(1 + \|\mathbf{U}(t)\|) + \frac{T^\hbar}{\mathcal{M}(\hbar)\Gamma(\hbar)} \mathfrak{V}(1 + \|\mathbf{U}(t)\|) \\ &\leq |\mathbf{U}_0| + \frac{1 - \hbar}{\mathcal{M}(\hbar)} \mathfrak{V} + \frac{T^\hbar}{\mathcal{M}(\hbar)\Gamma(\hbar)} \mathfrak{V} + \left[\frac{1 - \hbar}{\mathcal{M}(\hbar)} \mathfrak{V} + \frac{T^\hbar}{\mathcal{M}(\hbar)\Gamma(\hbar)} \mathfrak{V} \right] \varrho \\ &\leq \nabla_2 + \nabla_1 \varrho \leq \varrho. \end{aligned}$$

We have proven that $(\mathcal{U}\mathbb{B}_\varrho) \subset \mathbb{B}_\varrho$.

Next, to show that for the continuous operator \mathcal{U} , let us consider that $\{\mathbf{U}_n\}$ is a sequence $\ni \mathbf{U}_n \rightarrow \mathbf{U}$ in \mathbb{B}_ρ as $n \rightarrow \infty$; then, for all $t \in [0, T]$, we have the following

$$\begin{aligned} |(\mathcal{U}\mathbf{U}_n)(t) - (\mathcal{U}\mathbf{U})(t)| &\leq \frac{1 - \hbar}{\mathcal{M}(\hbar)} |\mathfrak{Z}(t, \mathbf{U}_n(t)) - \mathfrak{Z}(t, \mathbf{U}(t))| + \\ &\quad \frac{\hbar}{\mathcal{M}(\hbar)\Gamma(\hbar)} \int_0^t (t - \lambda)^{\hbar-1} |\mathfrak{Z}(\lambda, \mathbf{U}_n(\lambda)) - \mathfrak{Z}(\lambda, \mathbf{U}(\lambda))| d\lambda \\ &\leq \frac{1 - \hbar}{\mathcal{M}(\hbar)} \|\mathfrak{Z}(t, \mathbf{U}_n(t)) - \mathfrak{Z}(t, \mathbf{U}(t))\| \\ &\quad + \frac{T^\hbar}{\mathcal{M}(\hbar)\Gamma(\hbar)} \|\mathfrak{Z}(\lambda, \mathbf{U}_n(\lambda)) - \mathfrak{Z}(\lambda, \mathbf{U}(\lambda))\|. \end{aligned}$$

Hence, from the continuity of function \mathfrak{Z} , we obtain

$$\|(\mathcal{U}\mathbf{U}_n)(t) - (\mathcal{U}\mathbf{U})(t)\| \rightarrow 0 \quad \text{as } n \rightarrow \infty. \tag{14}$$

This shows that \mathcal{U} is continuous on \mathbb{B}_ρ . Finally, we present that $(\mathcal{U}\mathbb{B}_\rho)$ is a relatively compact operator. Because $(\mathcal{U}\mathbb{B}_\rho) \subset \mathbb{B}_\rho$, $(\mathcal{U}\mathbb{B}_\rho)$ is bounded uniformly. Further, we show the operator \mathcal{U} to be “equi-continuous” on \mathbb{B}_ρ . Consider $\mathbf{U} \in \mathbb{B}_\rho$ and that there is $t_1, t_2 \in [0, T]$ with $t_1 < t_2$; then, we have

$$\begin{aligned} \|\mathcal{U}\mathbf{U}(t_2) - \mathcal{U}\mathbf{U}(t_1)\| &\leq \frac{1 - \hbar}{\mathcal{M}(\hbar)} |\mathfrak{Z}(t_2, \mathbf{U}(t_2)) - \mathfrak{Z}(t_1, \mathbf{U}(t_1))| \\ &\quad + \frac{\hbar}{\mathcal{M}(\hbar)\Gamma(\hbar)} \left| \left[\int_0^{t_2} (t_2 - \lambda)^{\hbar-1} - \int_0^{t_1} (t_1 - \lambda)^{\hbar-1} \right] \mathfrak{Z}(\lambda, \mathbf{U}(\lambda)) d\lambda \right| \\ &\leq \frac{1 - \hbar}{\mathcal{M}(\hbar)} |\mathfrak{Z}(t_2, \mathbf{U}(t_2)) - \mathfrak{Z}(t_1, \mathbf{U}(t_1))| + \frac{\hbar}{\mathcal{M}(\hbar)} \frac{\mathcal{L}(\|\mathbf{U}\|)}{\Gamma(\hbar + 1)} (t_2^\hbar - t_1^\hbar). \end{aligned}$$

Apparently, the right side $\|\mathcal{U}\mathbf{U}(t_2) - \mathcal{U}\mathbf{U}(t_1)\| \rightarrow 0$ as $t_2 \rightarrow t_1$. In view of the Arzelà-Ascoli theorem, $(\mathcal{U}\mathbb{B}_\rho)$ is relatively compact, and thus, the operator is continuous completely. Therefore, the problem (1) has at least one solution.

Now, we discuss the uniqueness result for the suggested model (1), with the following assumption

$$0 \leq \left[1 - \frac{1 - \hbar}{\mathcal{M}(\hbar)} \varrho - \frac{\hbar T^\hbar}{\mathcal{M}(\hbar)\Gamma(\hbar)} \varrho \right]. \tag{15}$$

Suppose there exist other solutions such as $\mathbb{S}, \mathbb{V}, \mathbb{E}, \mathbb{I}, \mathbb{R}$; it holds that

$$\mathbb{S}(t) - \mathbb{S}_1(t) = \frac{1 - \hbar}{\mathcal{M}(\hbar)} (\mathbf{F}_1(t, \mathbb{S}) - \mathbf{F}_1(t, \mathbb{S}_1)) + \frac{\hbar}{\mathcal{M}(\hbar)\Gamma(\hbar)} \int_0^t (\mathbf{F}_1(\lambda, \mathbb{S}) - \mathbf{F}_1(\lambda, \mathbb{S}_1)) d\lambda, \tag{16}$$

using norm to Equation (16), we have

$$\begin{aligned} \|\mathbb{S} - \mathbb{S}_1\| &= \left\| \frac{1 - \hbar}{\mathcal{M}(\hbar)} (\mathbf{F}_1(t, \mathbb{S}) - \mathbf{F}_1(t, \mathbb{S}_1)) + \frac{\hbar}{\mathcal{M}(\hbar)\Gamma(\hbar)} \int_0^t (\mathbf{F}_1(\lambda, \mathbb{S}) - \mathbf{F}_1(\lambda, \mathbb{S}_1)) d\lambda \right\| \\ &\leq \frac{1 - \hbar}{\mathcal{M}(\hbar)} \varrho \|\mathbb{S} - \mathbb{S}_1\| + \frac{\hbar}{\mathcal{M}(\hbar)\Gamma(\hbar)} \varrho \|\mathbb{S} - \mathbb{S}_1\|. \end{aligned} \tag{17}$$

Therefore,

$$\|\mathbb{S} - \mathbb{S}_1\| \left[1 - \frac{1 - \hbar}{\mathcal{M}(\hbar)} \varrho - \frac{\hbar T^\hbar}{\mathcal{M}(\hbar)\Gamma(\hbar)} \varrho \right] \leq 0. \tag{18}$$

implies that $\mathbb{S} = \mathbb{S}_1$, if the inequality (15) holds. Considering that for the remaining compartments $\mathbb{V} = \mathbb{V}_1, \mathbb{E} = \mathbb{E}_1, \mathbb{I} = \mathbb{I}_1$, and $\mathbb{R} = \mathbb{R}_1$, the solution is unique. \square

Next, we show the UH stability for the suggested system (1).

Theorem 2. Consider $\mathcal{Z} \in \lambda$ to be a continuous function, let a constant $\mathcal{K} > 0 \ni |\mathcal{Z}(t, \mathbf{Q}) - \mathcal{Z}(t, \tilde{\mathbf{Q}})| \leq \mathcal{K}|\mathbf{Q} - \tilde{\mathbf{Q}}|, \forall t \in [0, T]$ and $\mathbf{Q} \in \lambda$ with $1 > \frac{(1-\hbar)\Gamma(\hbar)\mathcal{K} + \mathcal{K}T^\hbar}{\mathcal{M}(\hbar)\Gamma(\hbar)}$. Taking \mathbf{Q} and $\tilde{\mathbf{Q}}$ as the solution for Equation (6)

$${}^{ABC}D_t^\hbar \tilde{\mathbf{Q}}(t) = \mathcal{Z}(t, \tilde{\mathbf{Q}}(t)), \quad \tilde{\mathbf{Q}}(0) = \mathbf{Q}_0 + \varepsilon \geq 0, \tag{19}$$

where

$$\begin{cases} \tilde{\mathbf{Q}} = (\tilde{\mathcal{S}}, \tilde{\mathcal{V}}, \tilde{\mathcal{E}}, \tilde{\mathcal{I}}, \tilde{\mathcal{R}})^T, \\ \mathbf{Q}_0 + \varepsilon = (\mathcal{S}_0 + \varepsilon, \mathcal{V}_0 + \varepsilon, \mathcal{E}_0 + \varepsilon, \mathcal{I}_0 + \varepsilon, \mathcal{R}_0 + \varepsilon)^T, \\ \mathcal{Z}(t, \tilde{\mathbf{Q}}(t)) = \mathbf{F}_i(\tilde{\mathcal{S}}, \tilde{\mathcal{V}}, \tilde{\mathcal{E}}, \tilde{\mathcal{I}}, \tilde{\mathcal{R}})^T, \quad i = 1, 2, \dots, 5. \end{cases} \tag{20}$$

Then,

$$\|\mathbf{Q} - \tilde{\mathbf{Q}}\| \leq \left[1 - \frac{(1-\hbar)\Gamma(\hbar)\mathcal{K} + \mathcal{K}T^\hbar}{\mathcal{M}(\hbar)\Gamma(\hbar)} \right]^{-1} |\varepsilon|. \tag{21}$$

Proof. The solution of the given problem (6) and Equation (19) are equivalent to the integral Equation (8)

$$\tilde{\mathbf{Q}}(t) = \mathbf{Q}_0 + \varepsilon + \frac{1-\hbar}{\mathcal{M}(\hbar)} \mathcal{Z}(t, \tilde{\mathbf{Q}}(t)) + \frac{\hbar}{\mathcal{M}(\hbar)\Gamma(\hbar)} \int_0^t (t-\lambda)^{\hbar-1} \mathcal{Z}(\lambda, \tilde{\mathbf{Q}}(\lambda)) d\lambda, \tag{22}$$

every $t \in [0, T]$, we obtain

$$\begin{aligned} \|\mathbf{Q} - \tilde{\mathbf{Q}}\| &\leq |\varepsilon| + \frac{1-\hbar}{\mathcal{M}(\hbar)} |\mathcal{Z}(t, \mathbf{Q}(t)) - \mathcal{Z}(t, \tilde{\mathbf{Q}}(t))| \\ &\quad + \frac{\hbar}{\mathcal{M}(\hbar)\Gamma(\hbar)} \int_0^t (t-\lambda)^{\hbar-1} |\mathcal{Z}(\lambda, \mathbf{Q}(\lambda)) - \mathcal{Z}(\lambda, \tilde{\mathbf{Q}}(\lambda))| d\lambda \\ &\leq |\varepsilon| + \frac{1-\hbar}{\mathcal{M}(\hbar)} \mathcal{K} \|\mathbf{Q}(t) - \tilde{\mathbf{Q}}(t)\| + \frac{\hbar}{\mathcal{M}(\hbar)\Gamma(\hbar)} \int_0^t (t-\lambda)^{\hbar-1} \mathcal{K} \|\mathbf{Q}(\lambda) - \tilde{\mathbf{Q}}(\lambda)\| d\lambda \\ &\leq |\varepsilon| + \left[\frac{1-\hbar}{\mathcal{M}(\hbar)} + \frac{T^\hbar}{\mathcal{M}(\hbar)\Gamma(\hbar)} \right] \mathcal{K} \|\mathbf{Q} - \tilde{\mathbf{Q}}\|. \end{aligned}$$

Thus, we obtained

$$\|\mathbf{Q} - \tilde{\mathbf{Q}}\| \leq |\varepsilon| + \left[\frac{(1-\hbar)\Gamma(\hbar) + T^\hbar}{\mathcal{M}(\hbar)\Gamma(\hbar)} \right] \mathcal{K} \|\mathbf{Q} - \tilde{\mathbf{Q}}\|.$$

Hence,

$$\|\mathbf{Q} - \tilde{\mathbf{Q}}\| \leq \left[1 - \frac{(1-\hbar)\Gamma(\hbar)\mathcal{K} + \mathcal{K}T^\hbar}{\mathcal{M}(\hbar)\Gamma(\hbar)} \right]^{-1} |\varepsilon|.$$

Therefore, the theorem is proven. \square

4. Numerical Approach

Here, we explore a numerical technique for a given problem, wherein the time derivative is represented by a fractional derivative utilizing the generalized Mittag–Leffler (ML) kernel. Our investigation involved a numerical simulation employing an interpolation polynomial. To approximate the fractional-order integral using the AB (Adams–Bashforth) method, we applied the widely recognized Adams–Bashforth technique [56].

Using the initial conditions together with operator ${}^{ABC}I_0^\hbar$ and applying the scheme of on the given problem, we have

$$\begin{cases} \mathbb{S} - \mathbb{S}_0 &= {}^{AB}I_0^\hbar \mathbf{G}_1(\mathbb{S}, t), \\ \mathbb{V} - \mathbb{V}_0 &= {}^{AB}I_0^\hbar \mathbf{G}_2(\mathbb{V}, t), \\ \mathbb{E} - \mathbb{E}_0 &= {}^{AB}E_0^\hbar \mathbf{G}_3(\mathbb{E}, t), \\ \mathbb{I} - \mathbb{I}_0 &= {}^{AB}I_0^\hbar \mathbf{G}_4(\mathbb{I}, t), \\ \mathbb{R} - \mathbb{R}_0 &= {}^{AB}I_0^\hbar \mathbf{G}_5(\mathbb{R}, t), \end{cases} \tag{23}$$

which gives

$$\begin{aligned} \mathbb{S}(t) - \mathbb{S}_0 &= \frac{1 - \hbar}{\mathcal{M}(\hbar)} \mathbf{G}_1(\mathbb{S}(t), t) + \frac{\hbar}{\mathcal{M}(\hbar)\Gamma(\hbar)} \int_0^t (t - \lambda)^{\hbar-1} \mathbf{G}_1(\mathbb{S}(\lambda), \lambda) d\lambda, \\ \mathbb{V}(t) - \mathbb{V}_0 &= \frac{1 - \hbar}{\mathcal{M}(\hbar)} \mathbf{G}_2(\mathbb{V}(t), t) + \frac{\hbar}{\mathcal{M}(\hbar)\Gamma(\hbar)} \int_0^t (t - \lambda)^{\hbar-1} \mathbf{G}_2(\mathbb{V}(\lambda), \lambda) d\lambda, \\ \mathbb{E}(t) - \mathbb{E}_0 &= \frac{1 - \hbar}{\mathcal{M}(\hbar)} \mathbf{G}_3(\mathbb{E}(t), t) + \frac{\hbar}{\mathcal{M}(\hbar)\Gamma(\hbar)} \int_0^t (t - \lambda)^{\hbar-1} \mathbf{G}_3(\mathbb{E}(\lambda), \lambda) d\lambda, \\ \mathbb{I}(t) - \mathbb{I}_0 &= \frac{1 - \hbar}{\mathcal{M}(\hbar)} \mathbf{G}_4(\mathbb{I}(t), t) + \frac{\hbar}{\mathcal{M}(\hbar)\Gamma(\hbar)} \int_0^t (t - \lambda)^{\hbar-1} \mathbf{G}_4(\mathbb{I}(\lambda), \lambda) d\lambda, \\ \mathbb{R}(t) - \mathbb{R}_0 &= \frac{1 - \hbar}{\mathcal{M}(\hbar)} \mathbf{G}_5(\mathbb{R}(t), t) + \frac{\hbar}{\mathcal{M}(\hbar)\Gamma(\hbar)} \int_0^t (t - \lambda)^{\hbar-1} \mathbf{G}_5(\mathbb{R}(\lambda), \lambda) d\lambda, \end{aligned}$$

To develop an iterative scheme, we substitute $t = t_{i+1}$ for $\nu = 0, 1, 2, \dots$ into the above system

$$\begin{cases} \mathbb{S}(t_{\nu+1}) - \mathbb{S}(0) &= \frac{1-\hbar}{\mathcal{M}(\hbar)} \mathbf{G}_1(\mathbb{S}(t_\nu), t_\nu) + \frac{\hbar}{\mathcal{M}(\hbar)\Gamma(\hbar)} \sum_{i=0}^\nu \int_{t_i}^{t_{i+1}} (t_{\nu+1} - \lambda)^{\hbar-1} \mathbf{G}_1(\mathbb{S}(\lambda), \lambda) d\lambda, \\ \mathbb{V}(t_{\nu+1}) - \mathbb{V}(0) &= \frac{1-\hbar}{\mathcal{M}(\hbar)} \mathbf{G}_2(\mathbb{V}(t_\nu), t_\nu) + \frac{\hbar}{\mathcal{M}(\hbar)\Gamma(\hbar)} \sum_{i=0}^\nu \int_{t_i}^{t_{i+1}} (t_{\nu+1} - \lambda)^{\hbar-1} \mathbf{G}_2(\mathbb{V}(\lambda), \lambda) d\lambda, \\ \mathbb{E}(t_{\nu+1}) - \mathbb{E}(0) &= \frac{1-\hbar}{\mathcal{M}(\hbar)} \mathbf{G}_3(\mathbb{E}(t_\nu), t_\nu) + \frac{\hbar}{\mathcal{M}(\hbar)\Gamma(\hbar)} \sum_{i=0}^\nu \int_{t_i}^{t_{i+1}} (t_{\nu+1} - \lambda)^{\hbar-1} \mathbf{G}_3(\mathbb{E}(\lambda), \lambda) d\lambda, \\ \mathbb{I}(t_{\nu+1}) - \mathbb{I}(0) &= \frac{1-\hbar}{\mathcal{M}(\hbar)} \mathbf{G}_4(\mathbb{I}(t_\nu), t_\nu) + \frac{\hbar}{\mathcal{M}(\hbar)\Gamma(\hbar)} \sum_{i=0}^\nu \int_{t_i}^{t_{i+1}} (t_{\nu+1} - \lambda)^{\hbar-1} \mathbf{G}_4(\mathbb{I}(\lambda), \lambda) d\lambda, \\ \mathbb{R}(t_{\nu+1}) - \mathbb{R}(0) &= \frac{1-\hbar}{\mathcal{M}(\hbar)} \mathbf{G}_5(\mathbb{R}(t_\nu), t_\nu) + \frac{\hbar}{\mathcal{M}(\hbar)\Gamma(\hbar)} \sum_{i=0}^\nu \int_{t_i}^{t_{i+1}} (t_{\nu+1} - \lambda)^{\hbar-1} \mathbf{G}_5(\mathbb{R}(\lambda), \lambda) d\lambda, \end{cases}$$

To obtain the approximate functions $\mathbf{G}_1(\mathbb{S}(\lambda), \lambda)$, $\mathbf{G}_2(\mathbb{V}(\lambda), \lambda)$, $\mathbf{G}_3(\mathbb{E}(\lambda), \lambda)$, $\mathbf{G}_4(\mathbb{I}(\lambda), \lambda)$, and $\mathbf{G}_5(\mathbb{R}(\lambda), \lambda)$, a two-step interpolation polynomial is utilized, and the inside of the integral of the above equation on the interval $[t_\zeta, t_{\zeta+1}]$. We obtain

$$\begin{cases} \mathbf{G}_1(\mathbb{S}(\lambda), \lambda) &\cong \frac{\mathbf{G}_1(\mathbb{S}(t_\zeta), t_\zeta)}{\Delta} (t - t_{\zeta-1}) + \frac{\mathbf{G}_1(\mathbb{S}(t_{\zeta-1}), t_{\zeta-1})}{\Delta} (t - t_\zeta), \\ \mathbf{G}_2(\mathbb{V}(\lambda), \lambda) &\cong \frac{\mathbf{G}_2(\mathbb{V}(t_\zeta), t_\zeta)}{\Delta} (t - t_{\zeta-1}) + \frac{\mathbf{G}_2(\mathbb{V}(t_{\zeta-1}), t_{\zeta-1})}{\Delta} (t - t_\zeta), \\ \mathbf{G}_3(\mathbb{E}(\lambda), \lambda) &\cong \frac{\mathbf{G}_3(\mathbb{E}(t_\zeta), t_\zeta)}{\Delta} (t - t_{\zeta-1}) + \frac{\mathbf{G}_3(\mathbb{E}(t_{\zeta-1}), t_{\zeta-1})}{\Delta} (t - t_\zeta), \\ \mathbf{G}_4(\mathbb{I}(\lambda), \lambda) &\cong \frac{\mathbf{G}_4(\mathbb{I}(t_\zeta), t_\zeta)}{\Delta} (t - t_{\zeta-1}) + \frac{\mathbf{G}_4(\mathbb{I}(t_{\zeta-1}), t_{\zeta-1})}{\Delta} (t - t_\zeta), \\ \mathbf{G}_5(\mathbb{R}(\lambda), \lambda) &\cong \frac{\mathbf{G}_5(\mathbb{R}(t_\zeta), t_\zeta)}{\Delta} (t - t_{\zeta-1}) + \frac{\mathbf{G}_5(\mathbb{R}(t_{\zeta-1}), t_{\zeta-1})}{\Delta} (t - t_\zeta), \end{cases} \tag{24}$$

which gives

$$\begin{aligned}
 \mathbb{S}(t_{i+1}) &= \mathbb{S}(0) + \frac{1-\hbar}{\mathcal{M}(\hbar)} \mathbf{G}_1(\mathbb{S}(t_\nu), t_\nu) + \frac{\hbar}{\mathcal{M}(\hbar)\Gamma(\hbar)} \sum_{i=0}^{\nu} \left(\frac{\mathbf{G}_1(\mathbb{S}(t_\zeta), t_\zeta)}{\Delta} I_{\zeta-1, \hbar} \right. \\
 &\quad \left. + \frac{\mathbf{G}_1(\mathbb{S}(t_{\zeta-1}), t_{\zeta-1})}{\Delta} I_{\zeta, \hbar} \right), \\
 \mathbb{V}(t_{i+1}) &= \mathbb{V}(0) + \frac{1-\hbar}{\mathcal{M}(\hbar)} \mathbf{G}_2(\mathbb{V}(t_\nu), t_\nu) + \frac{\hbar}{\mathcal{M}(\hbar)\Gamma(\hbar)} \sum_{i=0}^{\nu} \left(\frac{\mathbf{G}_2(\mathbb{V}(t_\zeta), t_\zeta)}{\Delta} I_{\zeta-1, \hbar} \right. \\
 &\quad \left. + \frac{\mathbf{G}_2(\mathbb{V}(t_{\zeta-1}), t_{\zeta-1})}{\Delta} I_{\zeta, \hbar} \right), \\
 \mathbb{E}(t_{i+1}) &= \mathbb{E}(0) + \frac{1-\hbar}{\mathcal{M}(\hbar)} \mathbf{G}_3(\mathbb{E}(t_\nu), t_\nu) + \frac{\hbar}{\mathcal{M}(\hbar)\Gamma(\hbar)} \sum_{i=0}^{\nu} \left(\frac{\mathbf{G}_3(\mathbb{E}(t_\zeta), t_\zeta)}{\Delta} I_{\zeta-1, \hbar} \right. \\
 &\quad \left. + \frac{\mathbf{G}_3(\mathbb{E}(t_{\zeta-1}), t_{\zeta-1})}{\Delta} I_{\zeta, \hbar} \right), \\
 \mathbb{I}(t_{i+1}) &= \mathbb{I}(0) + \frac{1-\hbar}{\mathcal{M}(\hbar)} \mathbf{G}_4(\mathbb{I}(t_\nu), t_\nu) + \frac{\hbar}{\mathcal{M}(\hbar)\Gamma(\hbar)} \sum_{i=0}^{\nu} \left(\frac{\mathbf{G}_4(\mathbb{I}(t_\zeta), t_\zeta)}{\Delta} I_{\zeta-1, \hbar} \right. \\
 &\quad \left. + \frac{\mathbf{G}_4(\mathbb{I}(t_{\zeta-1}), t_{\zeta-1})}{\Delta} I_{\zeta, \hbar} \right), \\
 \mathbb{R}(t_{i+1}) &= \mathbb{R}(0) + \frac{1-\hbar}{\mathcal{M}(\hbar)} \mathbf{G}_5(\mathbb{R}(t_\nu), t_\nu) + \frac{\hbar}{\mathcal{M}(\hbar)\Gamma(\hbar)} \sum_{i=0}^{\nu} \left(\frac{\mathbf{G}_5(\mathbb{R}(t_\zeta), t_\zeta)}{\Delta} I_{\zeta-1, \hbar} \right. \\
 &\quad \left. + \frac{\mathbf{G}_5(\mathbb{R}(t_{\zeta-1}), t_{\zeta-1})}{\Delta} I_{\zeta, \hbar} \right),
 \end{aligned} \tag{25}$$

where

$$I_{\zeta-1, \hbar} = \int_{t_\zeta}^{t_{\zeta+1}} (t - t_{\zeta-1})(t_{i+1} - t)^{\hbar-1} dt, \quad I_{\zeta, \hbar} = \int_{t_\zeta}^{t_{\zeta+1}} (t - t_i)(t_{i+1} - t)^{\hbar-1} dt.$$

Here, we calculate the integrals $I_{\zeta-1, \hbar}$ and $I_{\zeta, \hbar}$ as follows

$$\begin{aligned}
 I_{\zeta-1, \hbar} &= -\frac{1}{\hbar} \left[(t_{\zeta+1} - t_{\zeta-1})(t_{i+1} - t_{\zeta+1})^\hbar - (t_\zeta - t_{\zeta-1})(t_{i+1} - t_\zeta)^\hbar \right] \\
 &\quad - \frac{1}{\hbar(\hbar-1)} \left[(t_{i+1} - t_{\zeta+1})^{\hbar+1} - (t_{i+1} - t_\zeta)^{\hbar+1} \right],
 \end{aligned}$$

and

$$I_{\zeta, \hbar} = -\frac{1}{\hbar} \left[(t_{\zeta+1} - t_i)(t_{i+1} - t_{\zeta+1})^\hbar \right] - \frac{1}{\hbar(\hbar-1)} \left[(t_{i+1} - t_{\zeta+1})^{\hbar+1} - (t_{i+1} - t_\zeta)^{\hbar+1} \right],$$

given that $t_\zeta = i\Delta$, one can easily find that

$$I_{\zeta-1, \hbar} = -\frac{\Delta^{\hbar+1}}{\hbar(\hbar+1)} \left[(l+1-\zeta)^\hbar (l-\zeta+2+\hbar) - (l-\zeta)^\hbar (l-\zeta+2+2\hbar) \right], \tag{26}$$

$$I_{\zeta, \hbar} = \frac{\Delta^{\hbar+1}}{\hbar(\hbar+1)} \left[(l+1-\zeta)^{\hbar+1} - (l-\zeta)^\hbar (l-\zeta+1+\hbar) \right]. \tag{27}$$

Substituting Equations (26) and (27) into Equation (25), we obtain

$$\begin{aligned} \mathbb{S}(t_{i+1}) &= \mathbb{S}(t_0) + \frac{(1-\hbar)}{\mathcal{M}(\hbar)} \left[\mathbf{G}_1(\mathbb{S}(t_i), t_i) \right] + \frac{\hbar}{\mathcal{M}(\hbar)} \sum_{i=0}^{\nu} \left(\frac{\mathbf{G}_1(\mathbb{S}(t_i), t_i)}{\Gamma(\hbar+2)} \right. \\ &\quad \times \Delta^\hbar \left[(\iota+1-\varsigma)^\hbar (\iota-\varsigma+2+\hbar) - (\iota-\varsigma)^\hbar (\iota-\varsigma+2+2\hbar) \right] \\ &\quad \left. - \frac{\mathbf{G}_1(\mathbb{S}(t_{\nu-1}), t_{\nu-1})}{\Gamma(\hbar+2)} \Delta^\hbar [(\iota+1-\varsigma)^{\hbar+1} - (\iota-\varsigma)^\hbar (\iota-\varsigma+1+\hbar)] \right), \end{aligned} \tag{28}$$

$$\begin{aligned} \mathbb{V}(t_{i+1}) &= \mathbb{V}(t_0) + \frac{(1-\hbar)}{\mathcal{M}(\hbar)} \left[\mathbf{G}_2(\mathbb{V}(t_i), t_i) \right] + \frac{\hbar}{\mathcal{M}(\hbar)} \sum_{i=0}^{\nu} \left(\frac{\mathbf{G}_2(\mathbb{V}(t_i), t_i)}{\Gamma(\hbar+2)} \right. \\ &\quad \times \Delta^\hbar \left[(\iota+1-\varsigma)^\hbar (\iota-\varsigma+2+\hbar) - (\iota-\varsigma)^\hbar (\iota-\varsigma+2+2\hbar) \right] \\ &\quad \left. - \frac{\mathbf{G}_2(\mathbb{V}(t_{\nu-1}), t_{\nu-1})}{\Gamma(\hbar+2)} \Delta^\hbar [(\iota+1-\varsigma)^{\hbar+1} - (\iota-\varsigma)^\hbar (\iota-\varsigma+1+\hbar)] \right), \end{aligned} \tag{29}$$

$$\begin{aligned} \mathbb{E}(t_{i+1}) &= \mathbb{E}(t_0) + \frac{(1-\hbar)}{\mathcal{M}(\hbar)} \left[\mathbf{G}_3(\mathbb{E}(t_i), t_i) \right] + \frac{\hbar}{\mathcal{M}(\hbar)} \sum_{i=0}^{\nu} \left(\frac{\mathbf{G}_3(\mathbb{E}(t_i), t_i)}{\Gamma(\hbar+2)} \right. \\ &\quad \times \Delta^\hbar \left[(\iota+1-\varsigma)^\hbar (\iota-\varsigma+2+\hbar) - (\iota-\varsigma)^\hbar (\iota-\varsigma+2+2\hbar) \right] \\ &\quad \left. - \frac{\mathbf{G}_3(\mathbb{E}(t_{\nu-1}), t_{\nu-1})}{\Gamma(\hbar+2)} \Delta^\hbar [(\iota+1-\varsigma)^{\hbar+1} - (\iota-\varsigma)^\hbar (\iota-\varsigma+1+\hbar)] \right), \end{aligned} \tag{30}$$

$$\begin{aligned} \mathbb{I}(t_{i+1}) &= \mathbb{I}(t_0) + \frac{(1-\hbar)}{\mathcal{M}(\hbar)} \left[\mathbf{G}_4(\mathbb{I}(t_i), t_i) \right] + \frac{\hbar}{\mathcal{M}(\hbar)} \sum_{i=0}^{\nu} \left(\frac{\mathbf{G}_4(\mathbb{I}(t_i), t_i)}{\Gamma(\hbar+2)} \right. \\ &\quad \times \Delta^\hbar \left[(\iota+1-\varsigma)^\hbar (\iota-\varsigma+2+\hbar) - (\iota-\varsigma)^\hbar (\iota-\varsigma+2+2\hbar) \right] \\ &\quad \left. - \frac{\mathbf{G}_4(\mathbb{I}(t_{\nu-1}), t_{\nu-1})}{\Gamma(\hbar+2)} \Delta^\hbar [(\iota+1-\varsigma)^{\hbar+1} - (\iota-\varsigma)^\hbar (\iota-\varsigma+1+\hbar)] \right), \end{aligned} \tag{31}$$

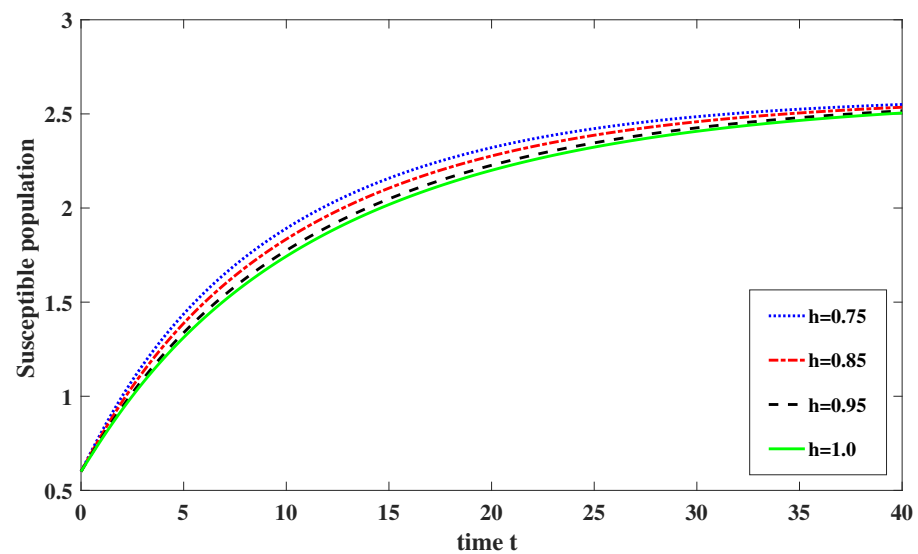
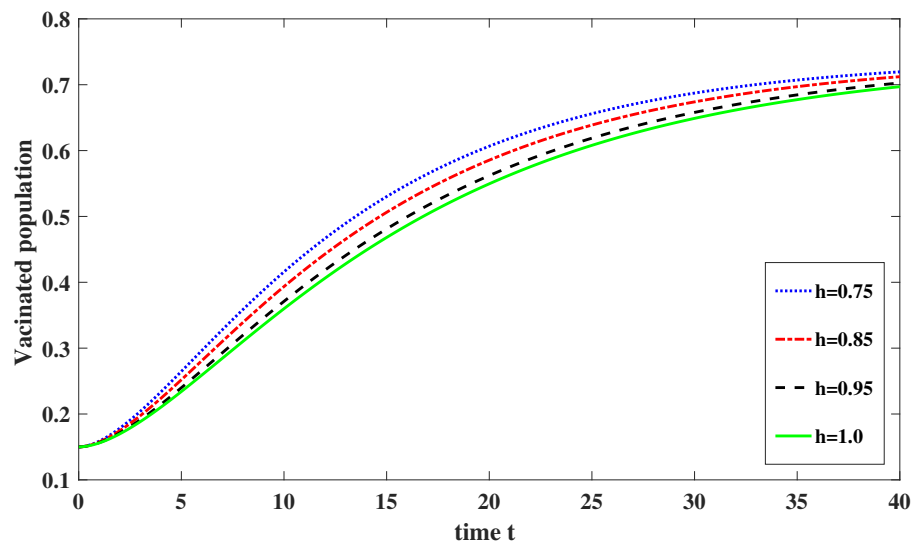
$$\begin{aligned} \mathbb{R}(t_{i+1}) &= \mathbb{R}(t_0) + \frac{(1-\hbar)}{\mathcal{M}(\hbar)} \left[\mathbf{G}_5(\mathbb{R}(t_i), t_i) \right] + \frac{\hbar}{\mathcal{M}(\hbar)} \sum_{i=0}^{\nu} \left(\frac{\mathbf{G}_5(\mathbb{R}(t_i), t_i)}{\Gamma(\hbar+2)} \right. \\ &\quad \times \Delta^\hbar \left[(\iota+1-\varsigma)^\hbar (\iota-\varsigma+2+\hbar) - (\iota-\varsigma)^\hbar (\iota-\varsigma+2+2\hbar) \right] \\ &\quad \left. - \frac{\mathbf{G}_5(\mathbb{R}(t_{\nu-1}), t_{\nu-1})}{\Gamma(\hbar+2)} \Delta^\hbar [(\iota+1-\varsigma)^{\hbar+1} - (\iota-\varsigma)^\hbar (\iota-\varsigma+1+\hbar)] \right). \end{aligned} \tag{32}$$

4.1. Numerical Simulation Results of the Model and Discussion

In this section, we present the numerical simulation in the form of a graphical representation for validating our required results at different fractional-order levels against the available data shown in Table 2, as well as the model’s initial conditions [55]. Figure 1 illustrates the temporal evolution of the susceptible class across different fractional order \hbar , wherein an initial increase was observed followed by stabilization. Notably, stability is achieved more rapidly at higher fractional orders. Similarly, the number of healthy individuals exhibits an upward trend as the vaccination rate increases, as depicted in Figure 2 for four distinct fractional orders.

Table 2. Values of the used parameters of the considered model (1).

Parameter	Value	Parameter	Value
\mathbb{S}	0.6	\mathbb{V}	0.17
\mathbb{E}	0.13	\mathbb{I}	0.05
\mathbb{R}	0.005	d_1	0.15
Θ	5	ϑ	0.2
d_2	0.12	ζ	0.3
α_1	0.8	α_2	3
γ_0	0.8	π	0.17
\varkappa	0.02	ς	0.7

**Figure 1.** Plots for $\mathbb{S}(t)$ at four different fractional orders h between 0, 1.**Figure 2.** Plots for $\mathbb{V}(t)$ at four different fractional orders h between 0, 1.

In this scenario, the exposed class experiences a rapid decline at lower fractional orders, followed by stabilization as a significant portion of the population becomes vaccinated, as depicted in Figure 3. Conversely, the infection class is effectively controlled, exhibiting a decline that contrasts with the trends observed in the susceptible and vaccinated classes, as illustrated in Figure 4. Lastly, Figure 5 shows the temporal evolution of the recovered class, which initially exhibits growth before gradually decaying and approaching stability across various fractional orders.

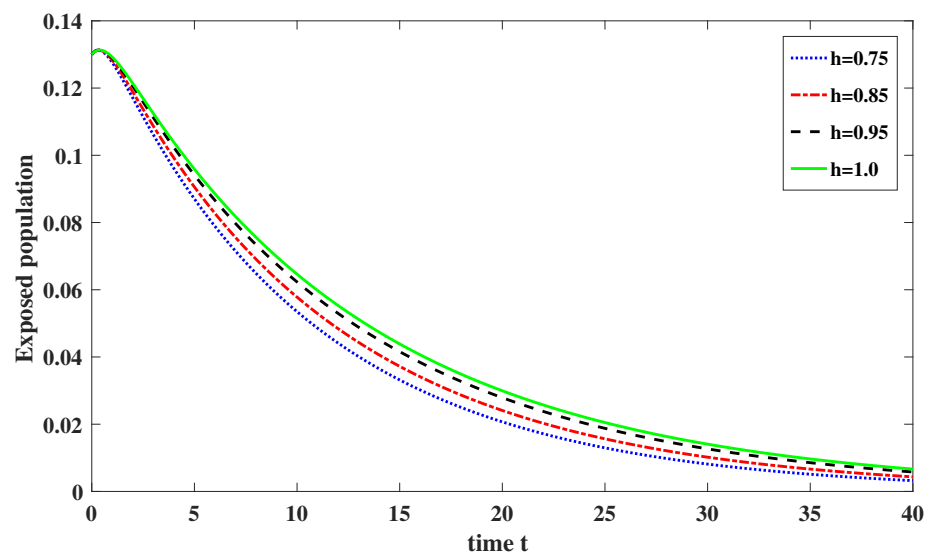


Figure 3. Plots for $\mathbb{E}(t)$ at four different fractional orders h between 0 and 1.

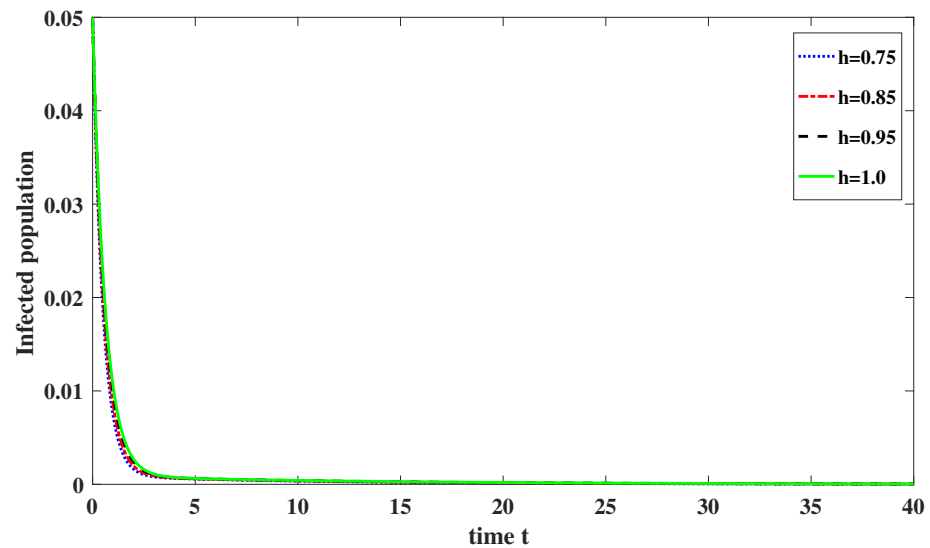


Figure 4. Plots for $\mathbb{I}(t)$ at four different fractional orders h between 0 and 1.

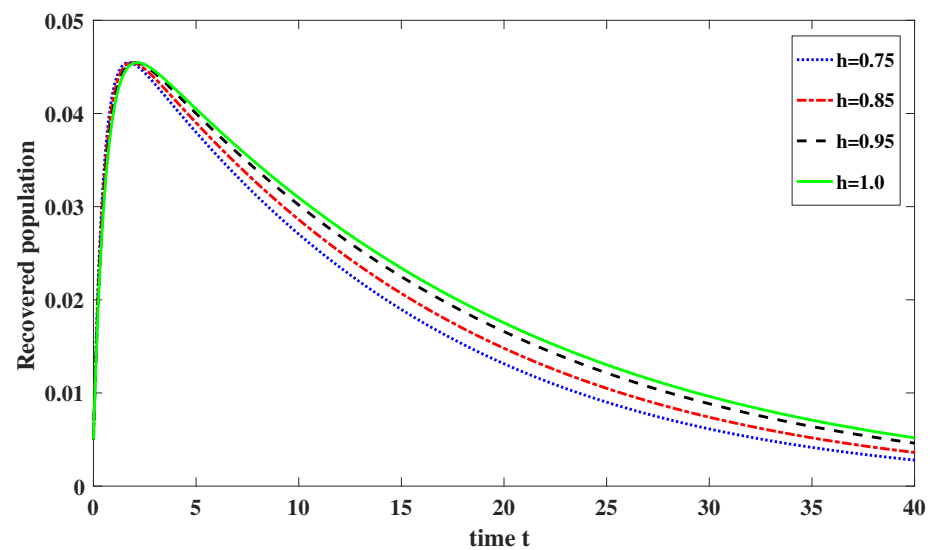


Figure 5. Plots for $\mathbb{R}(t)$ at four different fractional orders h between 0, 1, and $a = 0.145$.

In order to assess the sensitivity of the parameters and examine the dynamics of all five compartments prior to infection control, we conducted a series of experiments involving the manipulation of parameter values. The results of these experiments are presented in Table 3, which provides a comprehensive overview of the controlled and stable situation. The graphical representation of the data from Table 3 demonstrates the initial increase in infection rates, followed by a subsequent decline resulting from the vaccination of a larger proportion of individuals. This numerical simulation highlights the effectiveness of vaccination in mitigating the spread of infection and achieving a controlled and stable state.

Table 3. Values of the used parameters of the considered model (1).

Parameter	Value	Parameter	Value
S	0.6	V	0.17
E	0.13	I	0.05
R	0.005	d ₁	0.1
Θ	0.23	ϑ	0.2
d ₂	0.1	ζ	0.3
α ₁	0.2	α ₂	2
γ ₀	0.2	π	0.17
κ	0.02	ς	0.7

The graphical representation in Figure 6a–e for taking different fractional orders where as Figure 7a–e is another set of small fractional orders.

In Figures 8a–f and 9a–d, we presented a comparative analysis between the numerical scheme results and the series type solution obtained through the Laplace Adomian decomposition method (LADM) for all five compartments. This comparison was conducted for the first set of fractional orders, as well as the classical order 1. The graphs on the right-hand side depicted the results obtained through the LADM.

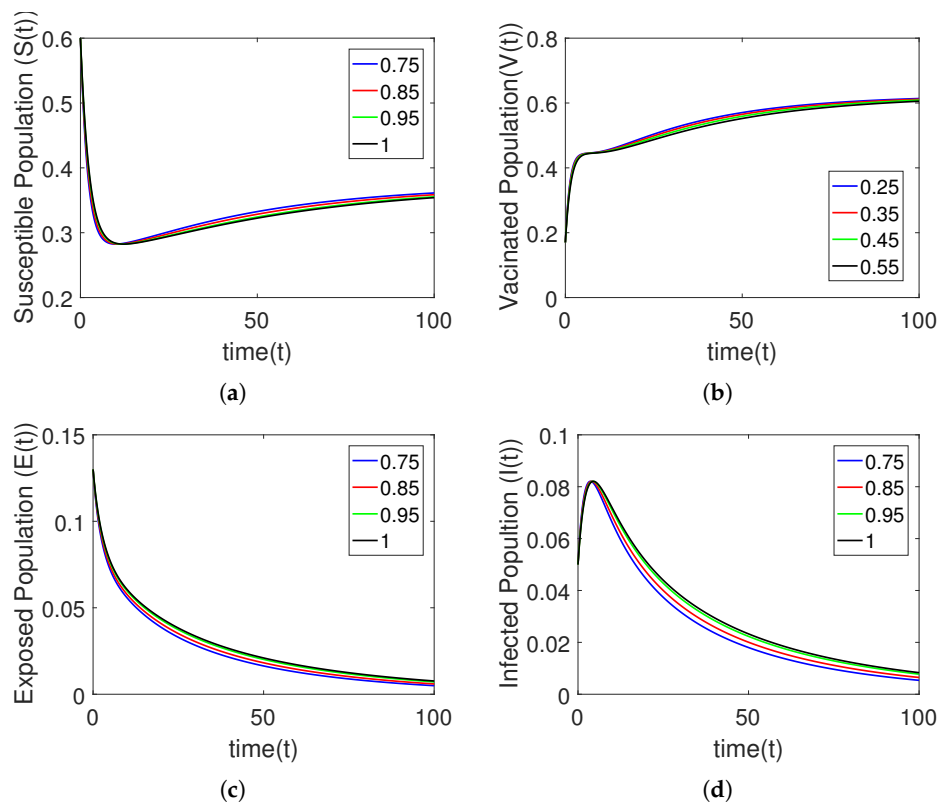


Figure 6. Cont.

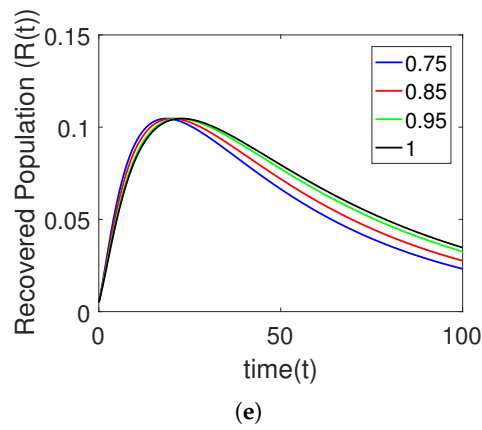


Figure 6. Plots for all five agents at four different fractional orders β between 0 and 1 for Table 2 data.

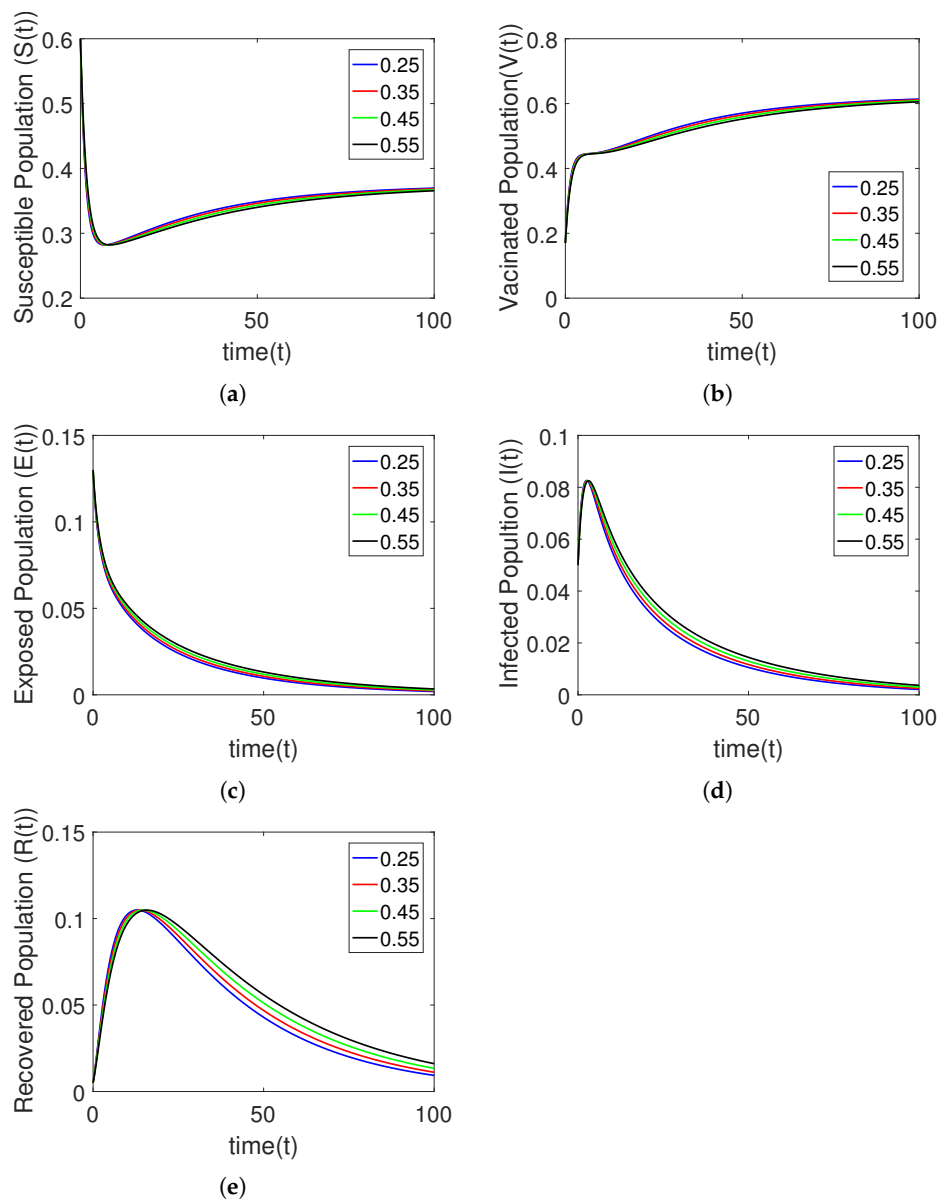


Figure 7. Plots for all five agents at four different fractional orders β between 0 and 1 for Table 2 data.

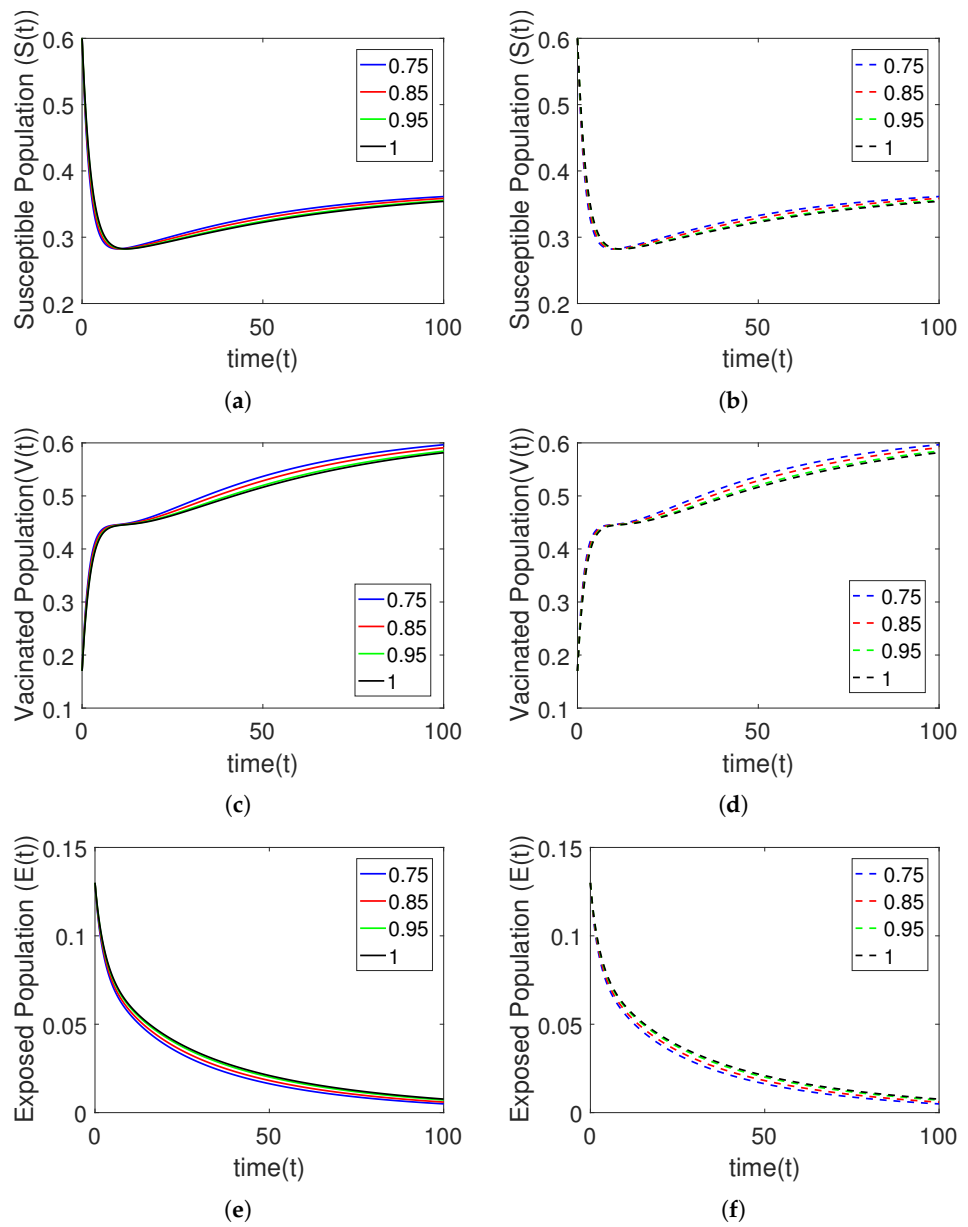


Figure 8. Comparison of obtained numerical scheme with LADM for first three agent on different orders h_i between 0 and 1 for Table 2 data.

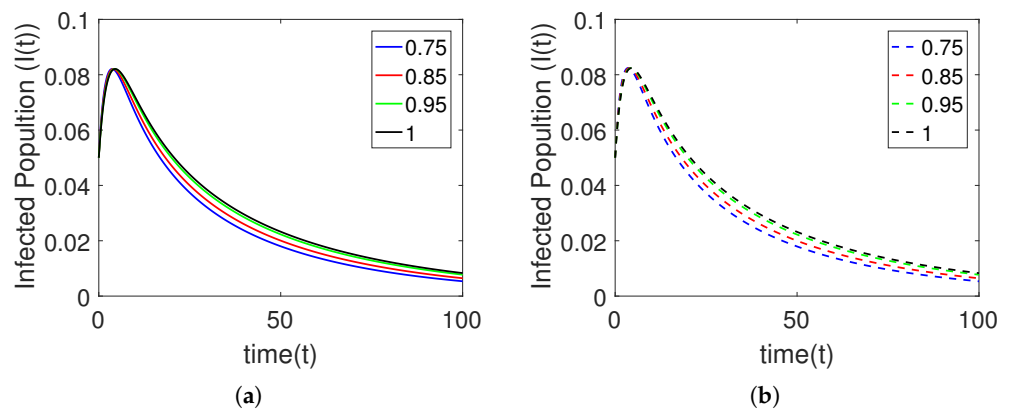


Figure 9. Cont.

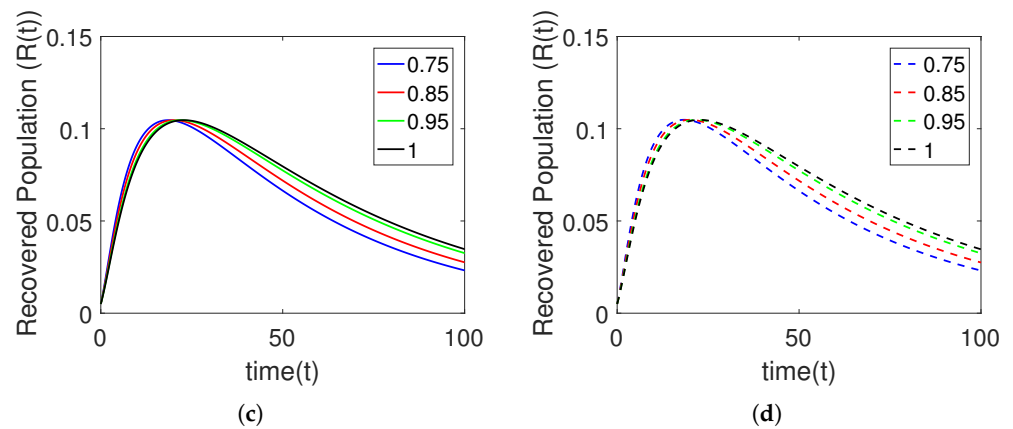


Figure 9. Comparison of obtained numerical scheme with LADM for last two agents on different orders β between 0 and 1 for Table 2 data.

In Figures 10a,f to 11c,d, we showed a comparative analysis between the numerical scheme results and the series type solution obtained through the Laplace Adomian decomposition method (LADM) for all five compartments. This comparison specifically focused on the second set of small fractional orders. The graphs on the right-hand side illustrated the results obtained through the LADM.

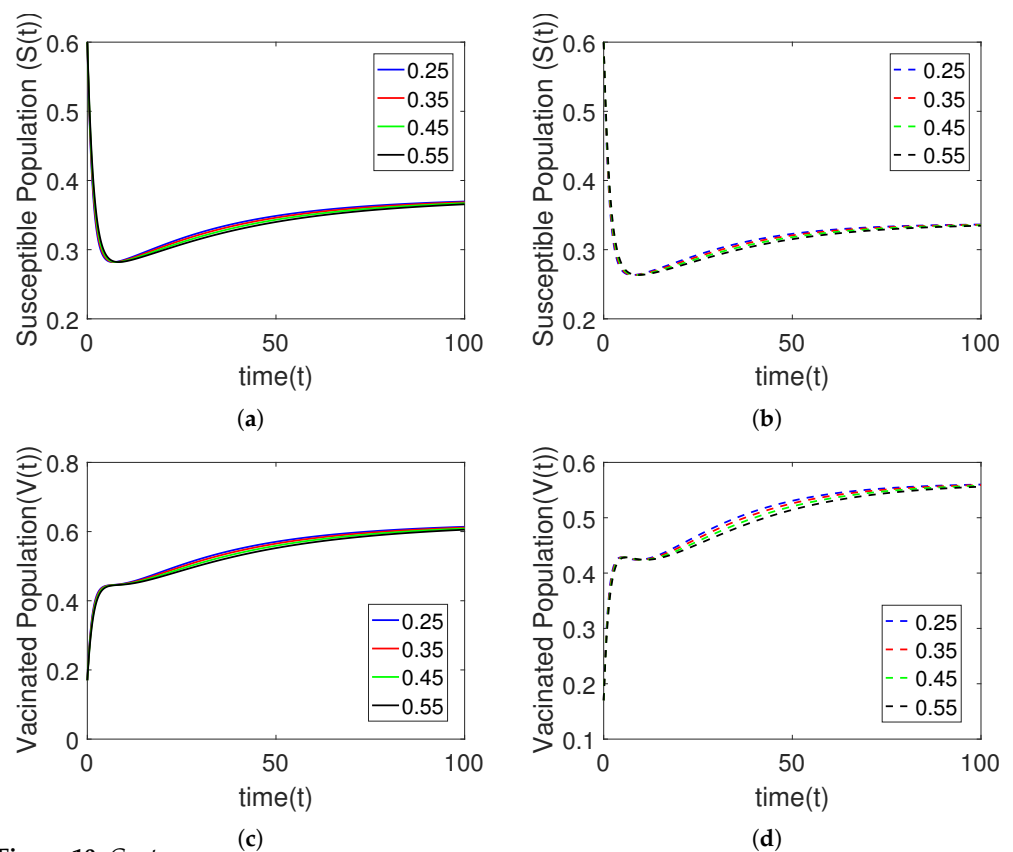


Figure 10. Cont.

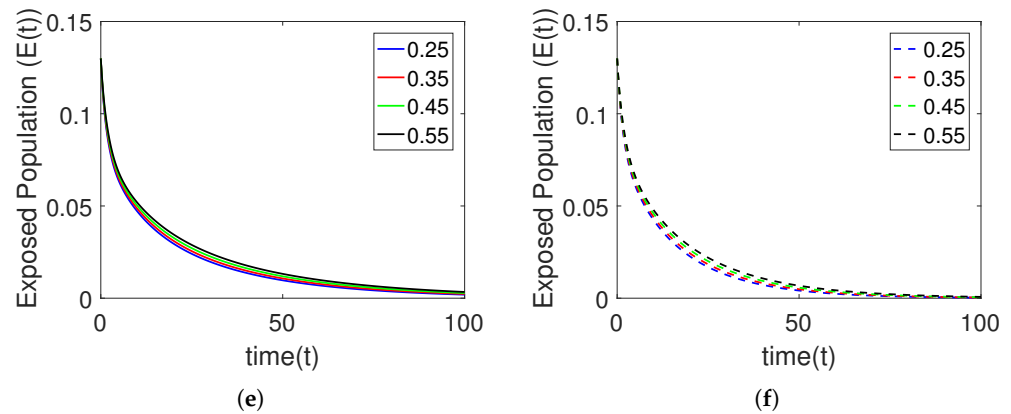


Figure 10. Comparison of obtained numerical scheme with LADM for first three agent on different orders h_i between 0 and 1 for Table 2 data.

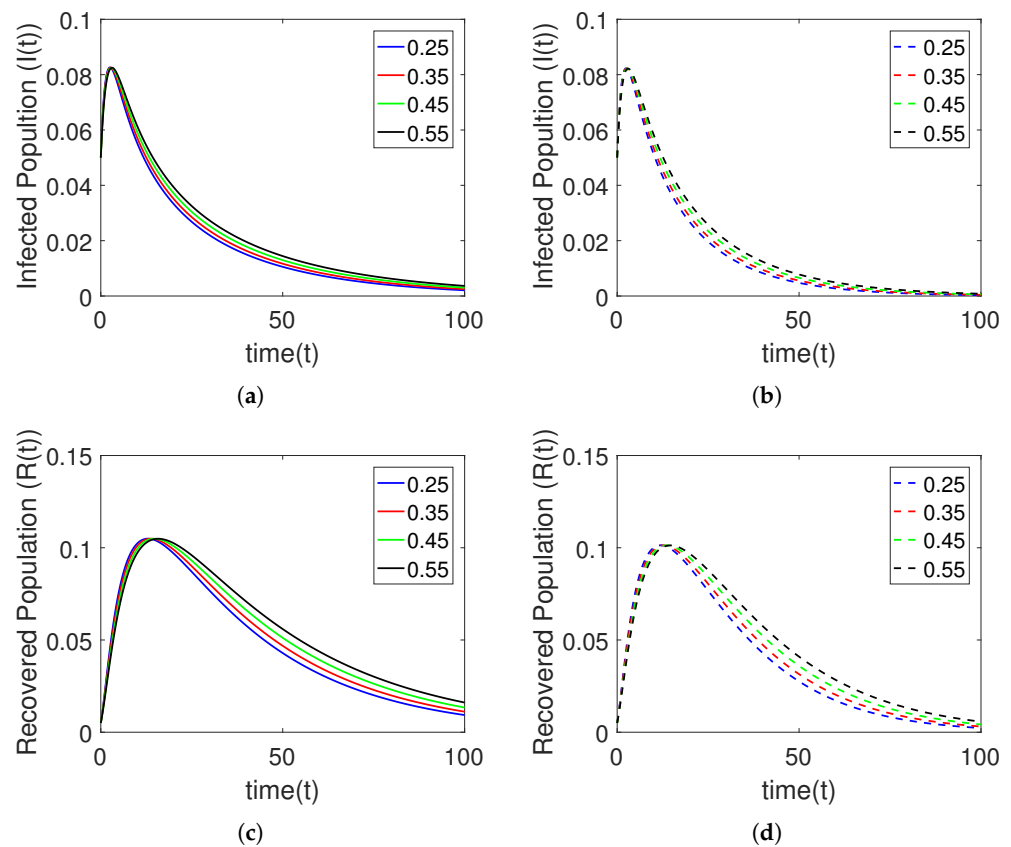


Figure 11. Comparison of obtained numerical scheme with LADM for last two agents on different orders h_i between 0 and 1 for Table 2 data.

4.2. Sensitivity of the Parameters

In this section, we introduce variations in parameter values to examine their impact on the dynamics of the five-compartmental model under consideration. These dynamics align with the characteristics observed in many epidemic models, wherein the susceptible class initially experiences a slight growth followed by a decline. The vaccinated and exposed classes exhibit an initial increase before declining and eventually stabilizing. On the other hand, the infected and recovered populations demonstrate an increase, reaching their peak point. The behavior of these classes is influenced by the inclusion of vaccination with different fractional orders, as illustrated in Figures 12a–e and 13a–e.

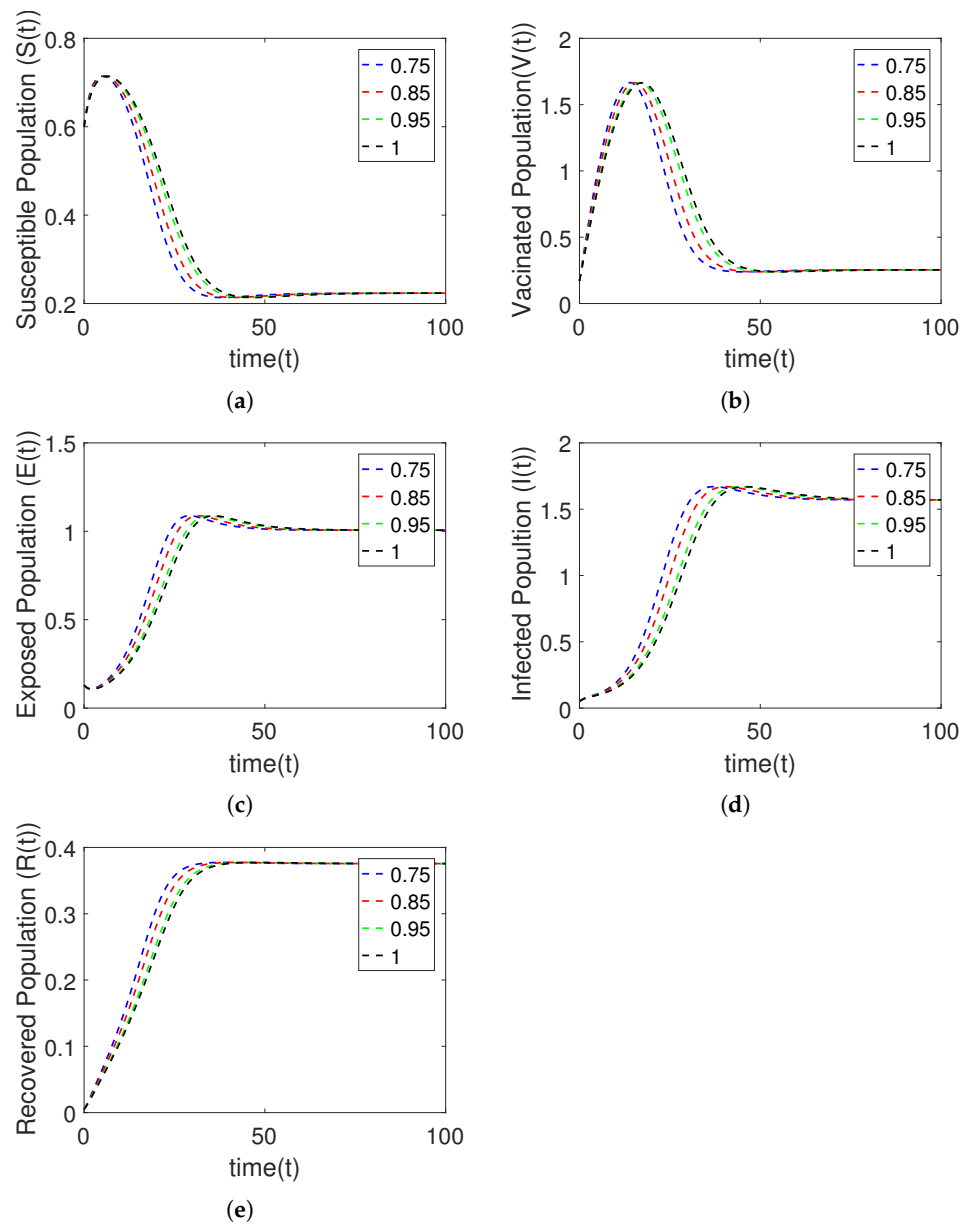


Figure 12. Plots for all five agents at four different fractional orders ℓ_i between 0 and 1 for Table 2 data by changing the values of ω and θ .

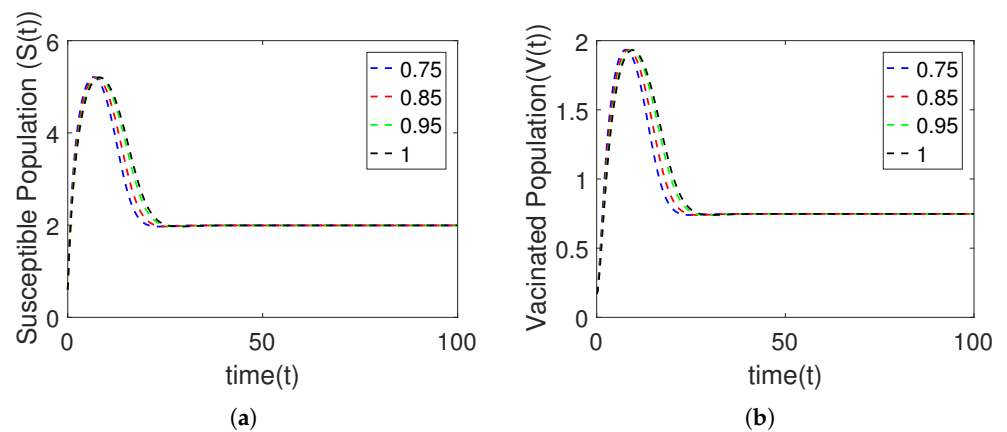


Figure 13. Cont.

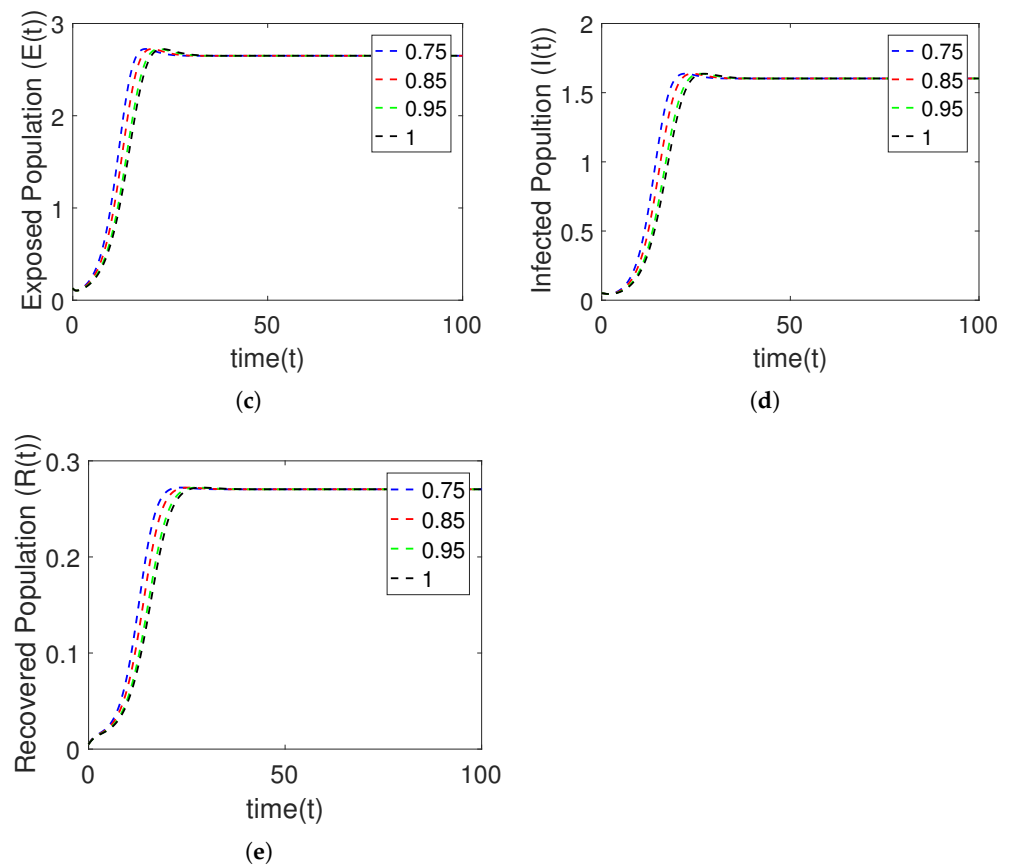


Figure 13. Plots for all five agents at four different fractional orders ι between 0 and 1 for Table 2 data by changing the values of ϑ .

5. Conclusions

The present manuscript offers a comprehensive investigation into the implications of tuberculosis (TB) on the human population. The study employs a five-compartment model that incorporates the utilization of the generalized ABC fractional operator. The dynamics of all compartments have been tested successfully on different fractional orders to validate the additional degree of freedom in selecting the derivative order. The fixed-point approach demonstrates the uniqueness and existence of solutions in the generalized format. Stability analysis of the model is performed using Ulam–Hyers’s stability techniques. An approximate solution for the model is obtained using the Adams–Bashforth technique. The study explores various fractional orders and iterative intervals, considering different initial conditions. Each curve is plotted for four different fractional orders and compared with the integer order. The analysis revealed that TB has a more significant impact on the adult population compared to the younger population. Moreover, the impact is lower for small fractional orders and higher for high fractional orders. In terms of stability, small fractional orders maintain high accuracy, whereas the opposite is true for high fractional orders. Furthermore, the numerical scheme is compared with the Laplace Adomian decomposition method for both fractional and classical orders.

Author Contributions: Conceptualization, S.A. and A.A.-B.; methodology, S.A.; software, S.P.; formal analysis, S.P., M.u.R., and A.A.-B.; investigation, S.P.; writing—original draft, S.A.; writing—review and editing, M.u.R. and A.A.-B.; supervision, M.u.R. All authors have read and agreed to the published version of the manuscript.

Funding: This study is supported via funding from Prince Sattam bin Abdulaziz University project number (PSAU/2023/R/1444).

Data Availability Statement: Not applicable.

Conflicts of Interest: The authors declare no conflict of interest.

References

- World Health Organisation. *Global Tuberculosis Report*; World Health Organisation: Geneva, Switzerland, 2018; p. 214.
- Wangari, I.M.; Stephen, D.; Stone, L. Backward bifurcation in epidemic models: Problems arising with aggregated bifurcation parameters. *Appl. Math. Model.* **2016**, *40*, 1669–1675. [[CrossRef](#)]
- Rie, A.V.; Warren, R.; Richardson, M.; Victor, T.C.; Gie, R.P.; Enarson, D.A.; Beyers, N.; Helden, P.D.V. Exogenous reinfection as a cause of recurrent tuberculosis after curative treatment. *N. Engl. J. Med.* **1999**, *341*, 1174–1179. [[PubMed](#)]
- Barberis, I.; Bragazzi, N.L.; Galluzzo, L.; Martini, M. The history of tuberculosis: From the first historical records to the isolation of Koch's bacillus. *J. Prev. Med. Hyg.* **2017**, *58*, E9. [[PubMed](#)]
- Adebisi, A.O. Mathematical Modeling of the Population Dynamics of Tuberculosis. Master Thesis, University of the Western Cape, Cape Town, South Africa, 2016.
- Khan, M.M.; Naqvi, H.; Thaver, D.; Prince, M. Epidemiology of suicide in Pakistan: Determining rates in six cities. *Arch. Suicide Res.* **2008**, *12*, 155–160. [[CrossRef](#)] [[PubMed](#)]
- Ullah, S.; Ullah, O.; Khan, M.K.; Gul, T. Optimal control analysis of tuberculosis (TB) with vaccination and treatment. *Eur. Phys. J. Plus* **2020**, *135*, 1–27. [[CrossRef](#)]
- Andersen, P.; Doherty, T.M. The success and failure of BCG—Implications for a novel tuberculosis vaccine. *Nat. Rev. Microbiol.* **2005**, *3*, 656–662. [[CrossRef](#)]
- Nadolinskaia, N.I.; Karpov, D.S.; Goncharenko, A.V. Vaccines against Tuberculosis: Problems and Prospects. *Appl. Biochem. Microbiol.* **2020**, *56*, 497–504. [[CrossRef](#)]
- Fine, P.E.M.; Carneiro, I.A.M.; Milstien, J.B.; Clements, C.J. *Issues Relating to the Use of BCG in Immunization Programmes: A Discussion Document (No. WHO/V and B/99.23)*; World Health Organization: Geneva, Switzerland, 1999.
- Anderson, R.M.; Robert, M.M. *Infectious Diseases of Humans: Dynamics and Control*; Oxford University Press: Oxford, UK, 1992.
- Feng, Z.; Chavez, C.C.; Capurro, A.F. A model for tuberculosis with exogenous reinfection. *Theor. Popul. Biol.* **2000**, *57*, 235–247. [[CrossRef](#)]
- Song, B.; Chavez, C.C.; Aparicio, J.P. Tuberculosis models with fast and slow dynamics: The role of close and casual contacts. *Math. Biosci.* **2002**, *180*, 187–205. [[CrossRef](#)]
- Bhunu, C.P.; Garira, W.; Mukandavire, Z.; Zimba, M. Tuberculosis transmission model with chemoprophylaxis and treatment. *Bull. Math. Biol.* **2008**, *70*, 1163–1191. [[CrossRef](#)]
- Khajanchi, S.; Das, D.K.; Kar, T.K. Dynamics of tuberculosis transmission with exogenous reinfections and endogenous reactivation. *Phys. Stat. Mech. Its Appl.* **2018**, *497*, 52–71. [[CrossRef](#)]
- Ullah, S.; Khan, M.A.; Farooq, M.; Gul, T. Modeling and analysis of tuberculosis (tb) in Khyber Pakhtunkhwa, Pakistan. *Math. Comput. Simul.* **2016**, *165*, 181–199. [[CrossRef](#)]
- Kar, T.K.; Mondal, P.K. Global dynamics of a tuberculosis epidemic model and the influence of backward bifurcation. *J. Math. Model. Algorithms* **2012**, *11*, 433–459. [[CrossRef](#)]
- Lakshmikantham, V.; Leela, S. Nagumo-type uniqueness result for fractional differential equations. *Nonlinear Anal.* **2009**, *71*, 2886–2889. [[CrossRef](#)]
- Podlubny, I. *Fractional Differential Equations: An Introduction to Fractional Derivatives, Fractional Differential Equations, to Methods of Their Solution and Some of Their Applications*; Elsevier: Amsterdam, The Netherlands, 1998.
- Sun, H.; Zhang, Y.; Baleanu, D.; Chen, W.; Chen, Y. A new collection of real world applications of fractional calculus in science and engineering. *Commun. Nonlinear Sci. Numer. Simul.* **2018**, *64*, 213–231. [[CrossRef](#)]
- Singh, J.; Kumar, D.; Hammouch, Z.; Atangana, A. A fractional epidemiological model for computer viruses pertaining to a new fractional derivative. *Appl. Math. Comput.* **2018**, *316*, 504–515. [[CrossRef](#)]
- Jarad, F.; Abdeljawad, T.; Hammouch, Z. On a class of ordinary differential equations in the frame of Atangana–Baleanu fractional derivative. *Chaos Solitons Fractals* **2018**, *117*, 16–20. [[CrossRef](#)]
- Valério, D.; Machado, J.T.; Kiryakova, V. Some pioneers of the applications of fractional calculus. *Fract. Calc. Appl. Anal.* **2014**, *17*, 552–578. [[CrossRef](#)]
- Liu, Z.; Li, X. Approximate Controllability of Fractional Evolution Systems with Riemann–Liouville Fractional Derivatives. *SIAM J. Control. Optim.* **2015**, *53*, 1920–1933. [[CrossRef](#)]
- Petráš, I. *Fractional-Order Nonlinear Systems: Modeling, Analysis and Simulation*; Springer Science & Business Media: Berlin/Heidelberg, Germany, 2011.
- Baleanu, D.; Diethelm, K.; Scalas, E.; Trujillo, J.J. *Fractional Calculus: Models and Numerical Methods*; World Scientific: London, UK, 2012; Volume 3.
- Al-Refai, M.; Luchko, Y. Maximum principle for the fractional diffusion equations with the Riemann–Liouville fractional derivative and its applications. *Fract. Calc. Appl. Anal.* **2014**, *17*, 483–498. [[CrossRef](#)]
- Sousa, E.; Li, C. A weighted finite difference method for the fractional diffusion equation based on the Riemann–Liouville derivative. *Appl. Numer. Math.* **2015**, *90*, 22–37. [[CrossRef](#)]

29. Atangana, A.; Baleanu, D. New fractional derivatives with nonlocal and non-singular kernel: Theory and application to heat transfer model. *Therm. Sci.* **2016**, *20*, 763–769. [[CrossRef](#)]
30. Djida, J.D.; Atangana, A.; Area, I. Numerical computation of a fractional derivative with non-local and non-singular kernel. *Math. Model. Nat. Phenom.* **2017**, *12*, 4–13. [[CrossRef](#)]
31. Pskhu, A.V. On the theory of the continual integro-differentiation operator. *Differ. Equ.* **2004**, *40*, 128–136. [[CrossRef](#)]
32. Jiang, X.; Li, J.; Li, B.; Yin, W.; Sun, L.; Chen, X. Bifurcation, chaos, and circuit realisation of a new four-dimensional memristor system. *Int. J. Nonlinear Sci. Numer. Simul.* **2022**. [[CrossRef](#)]
33. Pérez, A.G.C.; Oluyori, D.A. A model for COVID-19 and bacterial pneumonia coinfection with community-and hospital-acquired infections. *Math. Model. Numer. Simul. Appl.* **2022**, *2*, 197–210. [[CrossRef](#)]
34. Li, B.; Eskandari, Z.; Avazzadeh, Z. Strong resonance bifurcations for a discrete-time prey-predator model. *J. Appl. Math. Comput.* **2023**, *69*, 2421–2438. [[CrossRef](#)]
35. Rahman, M.u.; Arfan, M.; Baleanu, D. Piecewise fractional analysis of the migration effect in plant-pathogen-herbivore interactions. *Bull. Biomath.* **2023**, *1*, 1–23. [[CrossRef](#)]
36. Xu, C.; Rahman, M.u.; Fatima, B.; Karaca, Y. Theoretical and numerical investigation of complexities in fractional-order chaotic system having torus attractors. *Fractals* **2022**, *30*, 2250164. [[CrossRef](#)]
37. Abdeljawad, T.; Baleanu, D. Integration by parts and its applications of a new nonlocal fractional derivative with Mittag-Leffler nonsingular kernel. *J. Nonlinear Sci. Appl.* **2017**, *10*, 1098–1107. [[CrossRef](#)]
38. Ghanbari, B.; Atangana, A. A new application of fractional Atangana–Baleanu derivatives: Designing ABC-fractional masks in image processing. *Phys. Stat. Mech. Its Appl.* **2020**, *542*, 123516. [[CrossRef](#)]
39. Eskandari, Z.; Avazzadeh, Z.; Ghaziani, R.K.; Li, B. Dynamics and bifurcations of a discrete-time Lotka–Volterra model using nonstandard finite difference discretization method. In *Mathematical Methods in the Applied Sciences*; John Wiley & Sons, Ltd.: Hoboken, NJ, USA, 2022.
40. Li, B.; Liang, H.; Shi, L.; He, Q. Complex dynamics of Kopel model with nonsymmetric response between oligopolists. *Chaos Solitons Fractals* **2022**, *156*, 111860. [[CrossRef](#)]
41. Ahmad, S.; Qiu, D.; Rahman, M.u. Dynamics of a fractional-order COVID-19 model under the nonsingular kernel of Caputo–Fabrizio operator. *Math. Model. Numer. Simul. Appl.* **2022**, *2*, 228–243. [[CrossRef](#)]
42. Gómez-Aguilar, J.F. Irving–Mullineux oscillator via fractional derivatives with Mittag-Leffler kernel. *Chaos Solitons Fractals* **2017**, *95*, 179–186. [[CrossRef](#)]
43. Baleanu, D.; Fernandez, A. On some new properties of fractional derivatives with Mittag-Leffler kernel. *Commun. Nonlinear Sci. Numer. Simul.* **2018**, *59*, 444–462. [[CrossRef](#)]
44. Yavuz, M.; Ozdemir, N.; Baskonus, H.M. Solutions of partial differential equations using the fractional operator involving Mittag-Leffler kernel. *Eur. Phys. J. Plus* **2018**, *133*, 215. [[CrossRef](#)]
45. Li, B.; Liang, H.; He, Q. Multiple and generic bifurcation analysis of a discrete Hindmarsh–Rose model. *Chaos Solitons Fractals* **2021**, *146*, 110856. [[CrossRef](#)]
46. Mahmood, T.; Al-Duais, F.S.; Sun, M. Dynamics of Middle East Respiratory Syndrome Coronavirus (MERS-CoV) involving fractional derivative with Mittag-Leffler kernel. *Phys. Stat. Mech. Its Appl.* **2022**, *606*, 128144. [[CrossRef](#)] [[PubMed](#)]
47. Qu, H.; Liu, X.; Lu, X.; Rahman, M.u.; She, Z.H. Neural network method for solving nonlinear fractional advection-diffusion equation with spatiotemporal variable-order. *Chaos Solitons Fractals* **2022**, *156*, 111856. [[CrossRef](#)]
48. He, Q.; Xia, P.; Hu, C.; Li, B. Public information, actual intervention and inflation expectations. *Transform. Bus. Econ.* **2022**, *21*, 644–666.
49. Li, B.; Zhang, Y.; Li, X.; Eskandari, Z.; He, Q. Bifurcation analysis and complex dynamics of a Kopel triopoly model. *J. Comput. Appl. Math.* **2023**, *426*, 115089. [[CrossRef](#)]
50. Joshi, H.; Yavuz, M. Transition dynamics between a novel coinfection model of fractional-order for COVID-19 and tuberculosis via a treatment mechanism. *Eur. Phys. J. Plus* **2023**, *138*, 468. [[CrossRef](#)] [[PubMed](#)]
51. Shah, K.; Abdalla, B.; Abdeljawad, T.; Gul, R. Analysis of multipoint impulsive problem of fractional-order differential equations. *Bound. Value Probl.* **2023**, *2023*, 1. [[CrossRef](#)]
52. Yavuz, M.; Özköse, F.; Susam, M.; Kalidass, M. A new modeling of fractional-order and sensitivity analysis for hepatitis-b disease with real data. *Fractal Fract.* **2023**, *7*, 165. [[CrossRef](#)]
53. Asif, M.; Shah, K.; Abdalla, B.; Abdeljawad, T. Numerical solution of Bagley–Torvik equation including Atangana–Baleanu derivative arising in fluid mechanics. *Results Phys.* **2023**, *49*, 106468.
54. ur Rahman, M. Generalized fractal—Fractional order problems under non-singular Mittag-Leffler kernel. *Results Phys.* **2022**, *35*, 105346. [[CrossRef](#)]
55. Sulayman, F.; Abdullah, F.A.; Mohd, M.H. An SVEIRE model of tuberculosis to assess the effect of an imperfect vaccine and other exogenous factors. *Mathematics* **2021**, *9*, 327. [[CrossRef](#)]
56. Atangana, A.; Owolabi, K.M. New numerical approach for fractional differential equations. *Math. Model. Nat. Phenom.* **2018**, *13*, 3. [[CrossRef](#)]

Disclaimer/Publisher’s Note: The statements, opinions and data contained in all publications are solely those of the individual author(s) and contributor(s) and not of MDPI and/or the editor(s). MDPI and/or the editor(s) disclaim responsibility for any injury to people or property resulting from any ideas, methods, instructions or products referred to in the content.